8

Line, fibre and surface processes

8.1 Introduction

This chapter is concerned with the study of systems of fibres and of systems of surfaces or fragments of surfaces, distributed at random on the plane or in space. Interest is focused on general results that hold in the cases of stationarity or motion-invariance and on simple particular models. In this introductory section some illustrations and examples are discussed in order to motivate basic definitions.

Stochastic models of these systems are called *fibre processes* and *surface processes*; as in the term 'point process' no dependence on time is implied here. The theory of fibre and surface processes can be considered variously as belonging either to the theory of random closed sets or to the theory of random measures. As elsewhere in this book, in the case of stationarity one basic characteristic is the *intensity*, the mean fibre length per unit area (volume) for a planar (spatial) fibre process or the mean surface area per unit volume for a spatial surface process. Moreover, the constituent points of fibres and surfaces have associated directions (of tangents or normals) and these directions lead to a further important characteristic: the *rose of directions*.

Figures 8.1 and 8.2 display two realisations of irregular systems of lines in the plane, to be considered as samples of planar fibre processes. Figure 8.3 displays a spatial system of vessels which might be modelled by means of a spatial fibre process. The intensity here is the mean total fibre length per unit area or volume. The rose of directions summarises the spatial distribution of the collection of tangents to the fibres.

Planar fibre systems can also arise as planar sections of spatial surface systems such as the boundary of a three-dimensional Boolean model (see Chapter 3). There are stereological methods which enable estimation of characteristics of the original three-dimensional structure. The most important of these are the intensity (the mean surface area per unit volume) and the rose of directions.

Statistical investigation begins with estimation of intensity and rose of directions. A further stage considers the suitability of various fibre or surface process models for the sample. On

Stochastic Geometry and its Applications, Third Edition.
Sung Nok Chiu, Dietrich Stoyan, Wilfrid S. Kendall and Joseph Mecke.

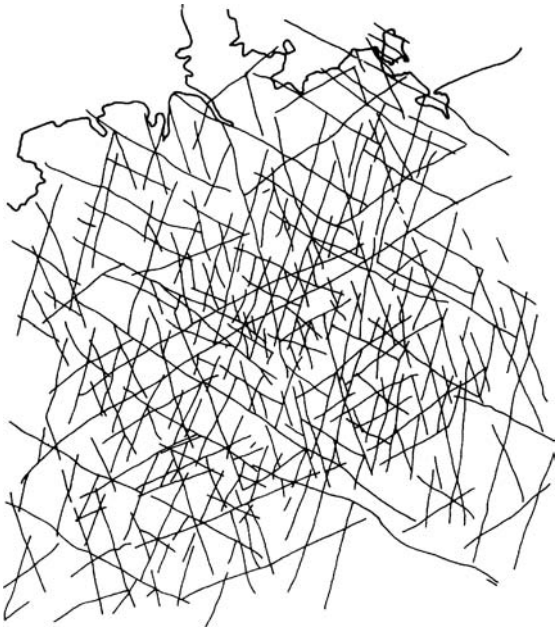

Figure 8.1 Distribution of linear fault zones in Central Europe (from Weber, 1977). The system of lines can be interpreted as a sample of a planar fibre process. A line process could also serve at least as a rough approximation; the pattern can be also interpreted as a sample of a geometrical network. Note that some of the fault zones end at other fault zones – so clearly there is interaction between them. The structure is clearly not isotropic. There are four dominating directions, ENE–WSW, NNE–SSW, NW–SE, ESE–WNW. The apparent lower intensity of fault zones in the northern region of the figure is due to incomplete information about that region. See the statistical analysis of fault lengths in Section 6.6.4, Figure 6.16.

occasion such a description can be suggestive of the manner in which the structures originated. Some examples of models are given below.

Figure 8.7 on p. 309 results from the simulation of a Poisson line process. This is an example of the class of *line processes* discussed in Section 8.2, which also can be considered as fibre processes. There is a considerable theory concerning such processes, which uses ideas of the theory of point processes. Higher-dimensional analogues are *plane*, *hyperplane* and general *flat processes* in $\mathbb{R}^3$ and $\mathbb{R}^d$. Figure 8.4 shows a sample of a plane process in $\mathbb{R}^3$. Also these structures are well understood as point processes in suitable representation spaces.

Random tessellations of space, as described in Chapter 9, yield fibre and surface processes, formed by their edge and facet systems.

Another particular class of fibre and surface processes comes from Boolean models.

Example 8.1. *Boolean fibre and surface process*

(a) *Planar Boolean fibre process*. Boolean models are characterised by the intensity of the underlying Poisson process and the distribution of the typical grain Ξ_0. In this example Ξ_0 is a random segment defined by a random point ξ on the unit circle and a positive random

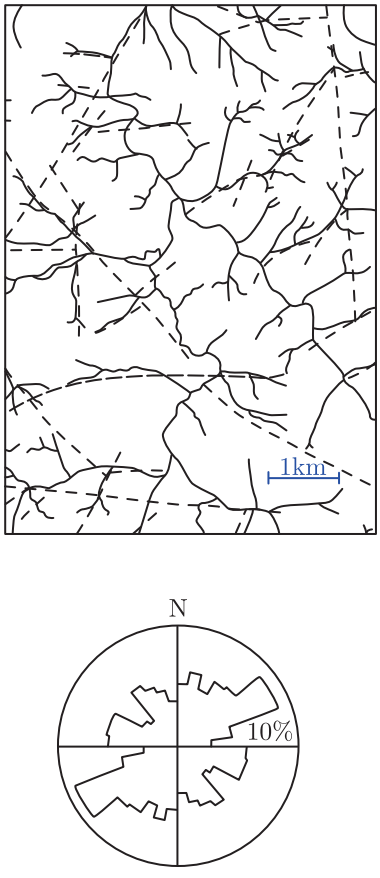

Figure 8.2 A part of the drainage network in the Eastern Erzgebirge (Saxony) and the corresponding rose of directions (derived from a larger region). The main flow direction in that region is SE–NW but the rose has its maximum at SW–NE. This is because of the large number of tributary rivers. The broken lines are fault lines.

variable l, representing orientation and length, respectively. The random set Ξ_0 is the line segment between o and $l\xi$. The corresponding Boolean model forms a fibre process in the plane. A simulated realisation of such a Boolean segment process with anisotropy is illustrated in Figure 8.5(a). To produce fibres from line segments, Kärkkäinen *et al.* (2012) deformed the line segments by dividing each segment into many short pieces and then 'shaking' them so that the angles between adjacent pieces follow a multivariate von Mises distribution (circular normal). Figure 8.5(b) shows a system of *von Mises fibres*, resulting from deforming the segments in Figure 8.5(a).

(b) *Boolean disc process*. If the typical grain Ξ_0 is a random isotropic two-dimensional disc in $\mathbb{R}^3$ of random radius R, then the corresponding Boolean model can be interpreted as a surface process in $\mathbb{R}^3$. This model and its generalisations are used in various papers in the context of discontinuities in engineering geology, such as structures arising from joints in

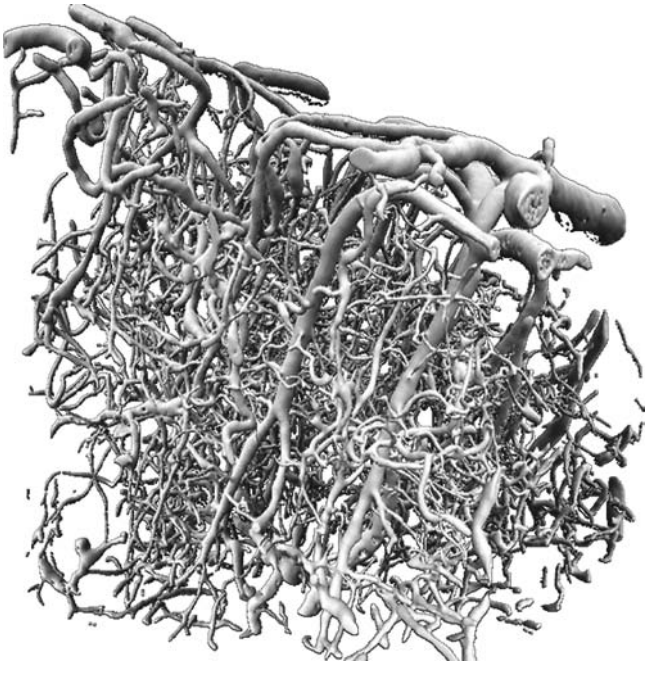

Figure 8.3 Scanning electron microscopic image of vasculature at the cortical surface. This may be regarded as a sample of a spatial fibre process with thick fibres. See Heinzer *et al.* (2006). Courtesy of R. Müller.

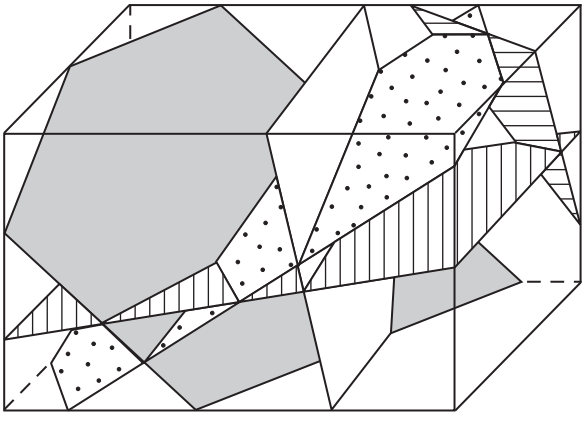

Figure 8.4 A sample of a plane process. This figure is also an example of a parallelepiped intersected by random planes. The intersection figures can be seen to have three, four, five, or six angles.

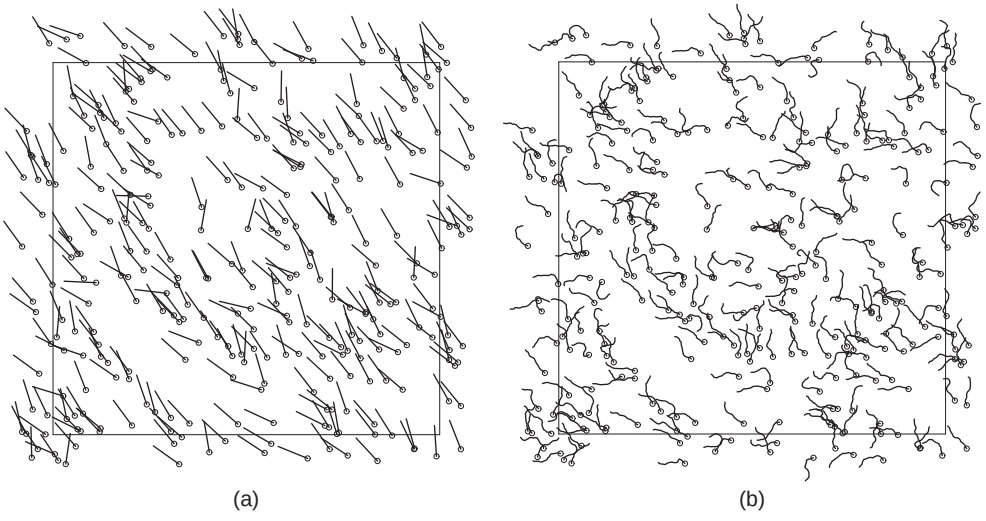

Figure 8.5 (a) A simulated realisation of an anisotropic Boolean segment process. All segments are of equal length. (b) A simulated system of von Mises fibres. The fibres result from the segments in part (a) by dividing the segments in 17 equal-length pieces the directions of which follow a multivariate von Mises distribution. See Kärkkäinen *et al.* (2012). Courtesy of S. Kärkkäinen.

rocks or from cracks in soil masses. Planar sections are visible on slopes or on outcrops and so *stereological* methods can be used to determine statistical characteristics of the underlying process; see Koschitzki (1980), Molek *et al.* (1981), Baecher (1983), Adler and Thovert (1999) and Thovert and Adler (2004), who speak about *fracture networks*. Berkowitz and Adler (1998) also study the secondary segment process consisting of the segments resulting from intersection of discs, which they call 'needles'.

This book confines itself to processes of *smooth* fibres and surfaces. Of course, there are more general theories. For example, surfaces are considered which are the boundaries of locally polyconvex sets, as in Weil (1997). Zähle (1982, 1983) and since then many others considered fibre and surface processes (and higher-dimensional generalisations) under much more relaxed regularity assumptions; Zähle (1982) is today a classic reference. The relatively stringent assumptions of Sections 8.3–8.5 are replaced in Zähle's work by the requirement that the sets involved are *Hausdorff-rectifiable* closed sets. This means that (together with a technical regularity condition) for such a set X the Hausdorff k-dimensional measure $h_k(X \cap K)$ is finite for any bounded subset K of $\mathbb{R}^d$; $k = 1$ for fibres, $k = d - 1$ for (hyper) surfaces. This more general theory is developed to give stereological formulae generalising (8.38) and (8.83) and to define direction distributions analogous to the roses of directions mentioned above and defined in Sections 8.3–8.5. Moreover, the formulae for intersections of fibre and surface processes can be generalised.

Zähle (1982, 1983) discussed a further avenue of generalisation: the case of fibre and surface processes on homogeneous Riemannian spaces. The most immediately applicable case of this is of fibre processes on the sphere.

Just as line and plane processes in $\mathbb{R}^2$ and $\mathbb{R}^3$ can be generalised to plane and flat processes in $\mathbb{R}^d$, so fibre and surface processes can be generalised to the *manifold processes* of Mecke (1981b). These are random systems of fragments of *manifolds* of fixed dimension embedded in some higher-dimensional Euclidean space $\mathbb{R}^d$. Here a manifold is a generalisation of a fibre or of a surface: it can be thought of as the solution set of some system of equations $f_1(x) = 0, \ldots, f_r(x) = 0$. Mecke studies the intersections of manifold processes with other manifold processes, and also intersections with fixed manifolds. Related second moments are considered in Jensen *et al.* (1990a,b) and Zähle (1990).

8.2 Flat processes

8.2.1 Introduction

This section considers flat processes as introduced in Section 4.8, that is, random systems of k-dimensional planes in $\mathbb{R}^d$. The particular case of $k = 1$ and $d = 2$, of lines in the plane, is considered in detail, as an example of a point process on a special representation space, which is here a cylinder in $\mathbb{R}^3$. Thus the theory of planar line processes becomes a special chapter in the general theory of point processes. The corresponding geometric structure leads to remarkable constraints on the variety of possible regular planar line processes. In the following this geometric structure is explored, and at the end of the section higher dimensional cases are also considered.

Point processes in other parameter spaces are considered in Small (1996), D. G. Kendall *et al.* (1999) and Kendall and Le (2010), in the context of statistics of shape; see also Chapter 8 of SKM95.

Practical applications tend to concern the special case of *Poisson line processes*. These generate tessellations of the plane and thus random polygons (as described in Section 9.5), and also provide useful models for random line probe sampling in stereology.

Before the formal introduction of the theory, the following remark on the construction of Poisson line processes in the plane may be enlightening.

One might seek to construct a Poisson line process as a particular 'Boolean model' with lines as grains. However, this does not lead to a reasonable structure. From the formal standpoint, a Boolean model has compact grains, but lines are unbounded sets and therefore not compact. The condition (3.2) is of course not satisfied for all K. A more constructive explanation of the problem is as follows. Assume that a Boolean model with lines as grains is given, where the probability for a line to be parallel to x_1-axis is zero. Let the intensity of the germ process be λ. Then almost all lines intersect the x_1-axis. For each integer n, the lines with germs in the strip $\{(x_1, x_2) : n \leq x_2 < n + 1\}$ produce a point process Φ_n of intensity λ on the x_1-axis. Consequently, the ensemble of all lines of the Boolean model generates a point process $\Phi = \bigcup_n \Phi_n$ on the x_1-axis of intersection points of *infinite* intensity.

8.2.2 Planar line processes

A representation space for lines in the plane

A *directed line* is a line together with a preferred direction along the line. The family of all undirected lines in the plane is denoted by $A(2, 1)$, and the family of all directed lines

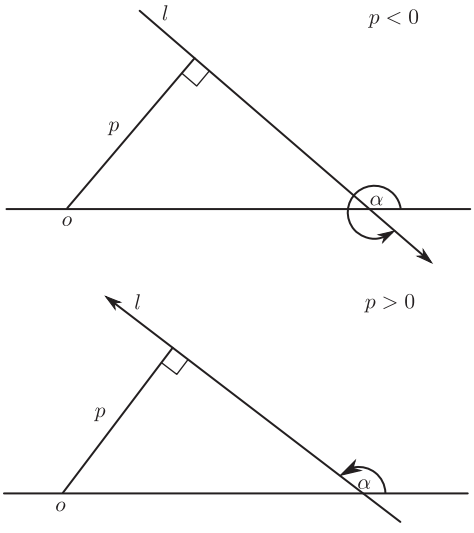

Figure 8.6 Construction of the representation space for directed lines in the plane. The two diagrams illustrate the cases of negative and positive signed perpendicular distance p.

by $A^*(2, 1)$. There is an obvious 2 : 1 correspondence between elements of $A^*(2, 1)$ and of $A(2, 1)$, obtained by ignoring direction.

Directed lines in the plane can be put into 1 : 1 correspondence with the set of points on the surface of a cylinder in $\mathbb{R}^3$. To see this, note that a convenient set of coordinates for a directed planar line ℓ is based on its perpendicular distance from the origin o and the angle that it makes with the x_1-axis.

In this approach, the first coordinate p is the *signed* perpendicular distance of ℓ from o; the sign is positive if o lies to the left of ℓ when looking in the direction of ℓ. The second coordinate α is the angle between ℓ and the x_1-axis, measured in an anticlockwise direction. Thus $p \in \mathbb{R}$ and $\alpha \in (0, 2\pi]$. The coordinatisation is illustrated by Figure 8.6. This supplies a 1 : 1 correspondence relating $A^*(2, 1)$ to the cylinder

$$\boldsymbol{C}^* = \{(\cos\alpha, \sin\alpha, p) \in \mathbb{R}^3 : p \in \mathbb{R}, \alpha \in (0, 2\pi]\}.$$

To each *undirected line* in $A(2, 1)$ there corresponds a pair of directed lines, and thus a pair of points in $\boldsymbol{C}^*$. The two points of every pair are reflections of each other in the origin. As representative of the undirected line the point is selected which is in the half-cylinder lying to one side of a fixed plane including the cylinder axis:

$$\boldsymbol{C} = \{(\cos\alpha, \sin\alpha, p) : p \in \mathbb{R}, \alpha \in (0, \pi]\}.$$

Note that as the angle α passes through 0 so the representative point jumps from one edge of the half-cylinder to the other, while the value of the p-coordinate is multiplied by -1.

Symmetries of the representation space

The representations described above depend on the particular choice of origin o and x_1-axis for the plane. The stochastic geometry of line processes must take account of such arbitrary choices, since they correspond to important symmetries in the representations.

The *motion-symmetry group* on $\boldsymbol{C}^*$ (or $\boldsymbol{C}$) is generated by those transformations of $A^*(2, 1)$ (or of $A(2, 1)$) that are induced by plane translations and rotations. The *translation-symmetry group* is composed of those transformations that are induced by plane translations alone. Point processes whose properties are invariant and measures in $\boldsymbol{C}^*$ (or $\boldsymbol{C}$) which are invariant under these groups are described as being respectively *motion-symmetric* or *translation-symmetric*. Up to a constant multiple there is only one measure on the representation cylinder $\boldsymbol{C}^*$ which is invariant under the motion-symmetry group, and measures which are invariant under the translation-symmetry group must have a special form. Line processes arising in stochastic geometry typically have properties which are at least invariant under the translation-symmetry group.

Discussion of the symmetries entails study of the transformations induced on the representation cylinder $\boldsymbol{C}^*$ by translations and rotations of the plane. From the construction of $\boldsymbol{C}^*$ it follows that a rotation through the angle β about the origin of the plane induces a rotation through the same angle of $\boldsymbol{C}^*$ around the cylinder axis, $(p, \alpha) \mapsto (p, \alpha + \beta)$. The effect of translations is seen by considering a translation through distance s parallel to the x_1-axis. Directions, and thus α, are unchanged but the perpendicular distance p of a line ℓ from the origin is changed to $p + s \sin\alpha$. Thus a translation induces a *shear* on the cylinder $\boldsymbol{C}^*$. More generally, consider the transformation $T_{(s,\gamma)}$ which corresponds to a translation through distance s in a direction that makes an angle γ with the x_1-axis. This will act on $\boldsymbol{C}^*$ by

$$T_{(s,\gamma)}(p, \alpha) = \big(p + s \sin(\alpha - \gamma), \alpha\big). \tag{8.1}$$

To see this, note that when $\boldsymbol{r}$ is a rotation about the origin through γ, then $\boldsymbol{r}T_{(s,\gamma)}\boldsymbol{r}^{-1}$ is a translation parallel to the x_1-axis.

So the symmetries of the rigid motions correspond to *rotations* of the cylinder and *vertical shears* along the cylinder's axis. Note that the rigid translational symmetries of $\boldsymbol{C}^*$ do not arise from the motion-symmetries of the plane underlying $A^*(2, 1)$.

Measures on the representation space

Line processes give rise to, and are controlled by, measures on the representation space $\boldsymbol{C}^*$, and analogously on $\boldsymbol{C}$. For example, Poisson directed-line processes can be defined as Poisson processes on $\boldsymbol{C}^*$; so their distributions are defined by their intensity measures on $\boldsymbol{C}^*$. Invariance properties holding for a line process lead to invariance properties for the corresponding measures, so the study of invariant measures is a necessary preliminary to the study of motion-invariant and stationary line processes.

Measures on $\boldsymbol{C}^*$ invariant under the translation-symmetry group induced by planar translations must be of a specific form. If invariant under the motion-symmetry group, they are unique up to a multiplicative factor.

Theorem 8.1. *(a) Suppose that μ is a locally finite measure on $\boldsymbol{C}^*$ which is invariant under the translation-symmetry group (plane-translation-invariant). Then μ is of the form*

$$\mu(\mathrm{d}p\,\mathrm{d}\alpha) = \nu_1(\mathrm{d}p) \cdot \kappa(\mathrm{d}\alpha) = \mathrm{d}p \cdot \kappa(\mathrm{d}\alpha) \tag{8.2}$$

for some finite measure κ on $(0, 2\pi]$, where ν_1 denotes as usual the one-dimensional Lebesgue measure.

(b) Suppose that μ is a locally finite measure on $\boldsymbol{C}^*$ which is invariant under the motion-symmetry group. Then μ is a constant multiple of Lebesgue measure on $\boldsymbol{C}^*$

$$\mu(\mathrm{d}p\,\mathrm{d}\alpha) = m\,\mathrm{d}p\,\mathrm{d}\alpha \tag{8.3}$$

for some constant m with $0 \le m < \infty$. If $m = 1$ then μ is the surface measure on $\boldsymbol{C}^*$ (regarding $\boldsymbol{C}^*$ as a cylinder in $\mathbb{R}^3$).

The measure with $m = 1$ is called *standard invariant measure*.

Theorem 8.1 can be proved by using differential forms (see Santaló, 1976). The famous encyclopaedia article by Crofton (1885) gives a heuristic argument which can be made precise as follows.

Proof. Let $T_{(s,\gamma)}$ be the translation through a distance s in a direction γ. For given α and β in $(0, 2\pi]$ consider the measure defined on intervals of $\mathbb{R}$ by

$$[a, b] \mapsto \mu([a, b] \times [\alpha, \beta]).$$

By translation-invariance of μ

$$\mu([a, b] \times [\alpha, \beta]) = \mu\big(T_{(s,\gamma)}([a, b] \times [\alpha, \beta])\big)$$

and by an approximation argument, it follows that

$$\begin{aligned}\mu([a, b] \times [\alpha, \beta]) &= \int_\alpha^\beta \mu\big(T_{(s,\gamma)}([a, b] \times \mathrm{d}\gamma)\big) \\ &= \int_\alpha^\beta \mu([s + a, s + b] \times \mathrm{d}\gamma) \\ &= \mu([s + a, s + b] \times [\alpha, \beta]).\end{aligned}$$

So μ is invariant under vertical shifts of the cylinder $\boldsymbol{C}^*$.

Formula (8.2) follows from general results on the uniqueness of translation-invariant measures on $\mathbb{R}$, while (8.3) follows from the implications of rotational invariance on the circle which is the base of $\boldsymbol{C}^*$. □

The invariant measures for $A(2, 1)$ can be derived (via the 2 : 1 correspondence) from those for $A^*(2, 1)$. Formulae (8.2) and (8.3) remain valid except that κ is now a measure on $(0, \pi]$.

Geometric arguments can also be used to derive formulae for the invariant measure of hitting sets. Define the *hitting set* of a compact subset K by

$$\mathcal{L}_K^* = \{\ell \in A^*(2, 1) : \ell \cap K \text{ is not empty}\}.$$

Theorem 8.2. *If μ is a motion-symmetric measure on $\boldsymbol{C}^*$, then*

$$\mu(\mathcal{L}_K^*) = 2mL(K) \qquad \text{for planar compact convex sets } K, \tag{8.4}$$

where $L(K)$ is the perimeter of K and m is the constant factor in (8.3).

Sketch of proof. If S is a line segment, then invariance considerations show that $\mu(\mathcal{L}_S^*)$ is proportional to the length of S, and does not depend on the orientation nor on the location of S. If K is a convex polygon of sides $S_1, \ldots, S_n$, then any ℓ in $\mathcal{L}_K^*$ intersects exactly 2 of the S_i, unless ℓ intersects the boundary of K at a vertex. Thus, using indicator functions,

$$2\mathbf{1}_{\mathcal{L}_K^*} \equiv \sum_i \mathbf{1}_{\mathcal{L}_{S_i}^*},$$

where $\equiv$ denotes equality of the indicator functions except on a set that is the finite union of hitting sets of points. Points $\boldsymbol{p}$ are segments of zero length and so $\mu(\mathcal{L}_{\boldsymbol{p}}^*) = 0$. Thus

$$2\mu(\mathcal{L}_K^*) = \sum_i \mu(\mathcal{L}_{S_i}^*) = \sum_i s_i \mu_1,$$

where s_i is the length of S_i and $\mu_1 = \mu(\mathcal{L}_{S_0}^*)$, in which S_0 is any segment of unit length. Integration shows that $\mu_1 = 2m$. A limiting argument yields Equation (8.4) for all convex compact K.

If K is the unit disc $B(o, 1)$, then

$$\mu(\mathcal{L}_{B(o,1)}^*) = 4\pi m.$$

An analogue of Theorem 8.2 holds for undirected lines, but $\mu(\mathcal{L}_K^*)$ has to be replaced by $\mu(\mathcal{L}_K)$, the set of all undirected lines hitting K, and the factor m by another constant, representing the ratio of the motion-symmetric μ to the Lebesgue measure on $\boldsymbol{C}$. The theorem for the undirected case can be generalised to higher-dimensional cases, where the lines are replaced by flats to obtain 'flat processes', see Schneider and Weil (2008, around Equation (4.27)).

One can also consider the evaluation of invariant μ on the hitting set of a finite union of line segments (the *Buffon–Sylvester problem*) and on general hitting sets of finite unions of convex bodies. Ambartzumian (1982) (note also there the appendix by A. Baddeley) described the full solution of this problem and generalisations.

Line processes as point processes on the representation space

A *line process* is a random collection of lines in the plane which is *locally finite*; only finitely many lines hit each compact planar set. It is convenient to consider directed line processes: results transfer easily to the undirected case. Formally, a directed line process is defined as a random collection of points in the representation space $\boldsymbol{C}^*$. The line process is locally finite exactly when the representing random collection is locally finite, hence a point process, on $\boldsymbol{C}^*$. Such point processes are particular cases of point processes on $\mathbb{R}^2$ because, as suggested by the parametrisation (p, α) of $\boldsymbol{C}^*$, the cylinder can be cut and embedded as the subset $\mathbb{R} \times (0, 2\pi]$ of $\mathbb{R}^2$. So the theory of line processes can be regarded as a special case of the theory of planar point processes as described in Chapters 2, 4 and 5.

The definitions of *stationary* and *motion-invariant* line processes are entirely analogous to those of stationary and motion-invariant point processes. The difference lies in the systematic replacement of the usual translation and motion groups in $\mathbb{R}^2$ by the translation-symmetry or motion-symmetry groups of $\boldsymbol{C}^*$ (or $\boldsymbol{C}$). Thus a line process $\Phi = \{\ell_1, \ell_2, \ldots\}$ is *stationary* if $\Phi_T = \{T\ell_1, T\ell_2, \ldots\}$ has the same distribution (considered as a line process) for every translation T of the plane, and this is to say that in the $\boldsymbol{C}^*$ representation the point process

$$\big\{\big(p(\ell_1) + s \cdot \sin(\alpha(\ell_1) + \gamma), \alpha(\ell_1)\big),\ \big(p(\ell_2) + s \cdot \sin(\alpha(\ell_2) + \gamma), \alpha(\ell_2)\big),\ \ldots\big\}$$

has the same point process distribution as

$$\big\{\big(p(\ell_1), \alpha(\ell_1)\big),\ \big(p(\ell_2), \alpha(\ell_2)\big),\ \ldots\big\} \tag{8.5}$$

for each s in $\mathbb{R}$ and γ in $(0, 2\pi]$.

Motion-invariant line processes have in addition the property that

$$\big\{\big(p(\ell_1), \alpha(\ell_1) + \gamma\big),\ \big(p(\ell_2), \alpha(\ell_2) + \gamma\big),\ \ldots\big\}$$

also has the same point process distribution as (8.5) for each γ in $(0, 2\pi]$, where the additions of angles $\alpha(\ell_k) + \gamma$ are interpreted modulo 2π.

The intensity measure and line density

A directed line process Φ, when regarded as a point process $\Phi_{\boldsymbol{C}^*}$ on $\boldsymbol{C}^*$, yields an *intensity measure* $\Lambda_{\boldsymbol{C}^*}$ on $\boldsymbol{C}^*$:

$$\Lambda_{\boldsymbol{C}^*}(A) = \mathbf{E}\big(\#\{(p, \alpha) \in \Phi_{\boldsymbol{C}^*} \cap A\}\big) \qquad \text{for all Borel sets } A \text{ of } \boldsymbol{C}^*. \tag{8.6}$$

If Φ is stationary then $\Lambda_{\boldsymbol{C}^*}$ is translation-symmetric, and if $\Lambda_{\boldsymbol{C}^*}$ is locally finite then Formula (8.2) can be applied to obtain

$$\Lambda_{\boldsymbol{C}^*}\big(\mathrm{d}(p, \alpha)\big) = \lambda\, \mathrm{d}p \cdot \mathscr{R}(\mathrm{d}\alpha), \tag{8.7}$$

where λ is a constant, the interpretation of which will become clear below by Formula (8.11), and $\mathscr{R}$ is a probability measure on $(0, 2\pi]$, called the *rose of directions* of Φ. The rose of directions can be interpreted as the distribution of direction of the typical (or, so to speak, a randomly selected) line of Φ.

In the case of motion-invariance, Formula (8.3) can be applied to obtain

$$\Lambda_{\boldsymbol{C}^*}\big(\mathrm{d}(p, \alpha)\big) = \lambda\, \mathrm{d}p \cdot \frac{\mathrm{d}\alpha}{2\pi}. \tag{8.8}$$

The constant $\lambda/(2\pi)$ is then the intensity of the representing point process $\Phi_{\boldsymbol{C}^*}$ with respect to the standard invariant measure $\mathrm{d}p \cdot \mathrm{d}\alpha$.

Now the meaning of the λ in (8.7) and (8.8) is explained as follows. If the line process Φ is stationary, then invariance arguments can be applied to the line length measure

$$\Lambda(B) = \mathbf{E}\left(\sum_{\ell \in \Phi} \nu_{1,\ell}(\ell \cap B)\right) \qquad \text{for all planar Borel sets } B, \tag{8.9}$$

where $\nu_{1,\ell}$ is the Lebesgue measure on the line ℓ. That is to say, $\Lambda(B)$ is the mean total length of all line pieces of Φ in B. Because Λ is a translation-invariant measure on $\mathbb{R}^2$, there is a

constant L_A such that

$$\Lambda(B) = L_A\, \nu_2(B) \qquad \text{for all planar Borel sets } B. \tag{8.10}$$

Thus, L_A is the mean line length per unit area.

The relationship of L_A to λ can be determined by inserting in Formula (8.10) a special set B, namely, $B = B(o, 1)$, which yields, using the Campbell theorem,

$$\pi L_A = \Lambda\big(B(o,1)\big) = \mathbf{E}\left(\sum_{\ell\in\Phi} \nu_{1,\ell}\big(\ell \cap B(o,1)\big)\right) = \mathbf{E}\left(\sum_{(p,\alpha)\in\Phi_{\boldsymbol{C}^*}:|p|\le 1} 2\sqrt{1-p^2}\right)$$

$$= 2\int_{(0,2\pi]}\int_{[-1,1]} \sqrt{1-p^2}\,\Lambda_{\boldsymbol{C}^*}\big(\mathrm{d}(p,\alpha)\big) = 2\lambda\int_{-1}^{1}\sqrt{1-p^2}\,\mathrm{d}p = \lambda\pi,$$

since the length of the chord in $B(o, 1)$ of a line of distance p from o is $2\sqrt{1-p^2}$. Thus

$$\lambda = L_A \tag{8.11}$$

is obtained.

Undirected line processes satisfy similar formulae, but subject to replacement of $\mathrm{d}p \cdot \mathrm{d}\alpha/(2\pi)$ in Formula (8.8) by $\mathrm{d}p \cdot \mathrm{d}\alpha/\pi$, and conversion of the rose of directions $\mathscr{R}$ into a distribution on $(0, \pi]$. Also here Equation (8.11) holds.

Since line processes can be regarded as point processes on the representation space, the definition of second and higher *moment measures* is straightforward. These concepts, though playing an important rôle in the general theory of line processes (see e.g. Ambartzumian, 1990, pp. 256–61, and Daley and Vere-Jones, 2008, pp. 477–82), will not be discussed further here.

Poisson line processes

A Poisson line process is the line process produced by a Poisson process on $\boldsymbol{C}^*$. Consequently it is characterised completely by its intensity measure $\Lambda_{\boldsymbol{C}^*}$. Thus stationary Poisson line processes are characterised by the line density L_A and the rose of directions $\mathscr{R}$. Moreover, stationary Poisson line processes are motion-invariant precisely when the rose of directions is the uniform probability measure on $(0, 2\pi]$.

Poisson line processes provide examples of stationary line processes which are free of parallel lines, since a Poisson point process on $\boldsymbol{C}^*$ with intensity $L_A\,\mathrm{d}p \cdot \mathscr{R}(\mathrm{d}\alpha)$ can have no more than one point per vertical line when the rose of directions $\mathscr{R}$ is diffuse. All this remains true for the case of undirected lines except that $\mathscr{R}$ is then a distribution on $(0, \pi]$.

Example 8.2. *The motion-invariant Poisson line process*
Let Φ be a motion-invariant directed Poisson line process of line density L_A. Then the number of lines of Φ hitting a convex body K is of Poisson distribution of mean

$$\mu_K = \frac{L_A}{\pi} \cdot L(K), \tag{8.12}$$

where $L(K)$ is the perimeter of K.

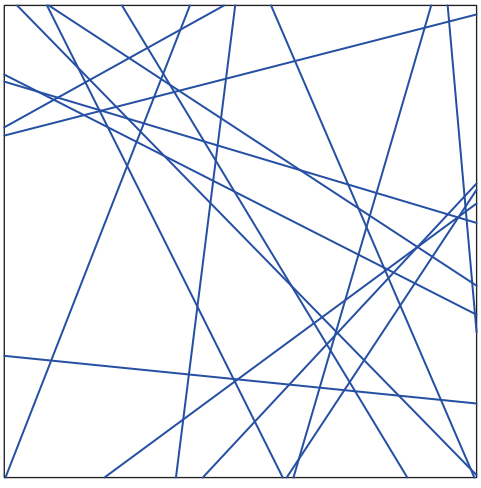

Figure 8.7 A simulated realisation of a Poisson line process of intensity $L_A = 15$ in $[0, 1]^2$.

The Poisson distribution is established by noting that the number of lines hitting K is precisely the number of representing points lying in a certain subset of $\boldsymbol{C}^*$. The value for the mean is derived by applying Theorem 8.2 to the intensity measure of $\Phi_{\boldsymbol{C}^*}$, which is $\Lambda_{\boldsymbol{C}^*}\big(\mathrm{d}(p, \alpha)\big) = L_A \, \mathrm{d}p \cdot \mathrm{d}\alpha/(2\pi)$.

For undirected lines Formula (8.12) is also true.

The *simulation* of a motion-invariant undirected Poisson process of line density L_A usually consists in determining random lines that hit some convex window W. The number of lines is obtained by sampling a Poisson variable with mean $\mu_W = L_A \cdot L(W)/\pi$ and the lines then are obtained as points uniformly distributed in the counterpart of W in $\boldsymbol{C}^*$. One can also take a disc $B(o, r)$ containing W, simulate random lines hitting $B(o, r)$ and reject those lines that do not hit W.

A simulated realisation of a motion-invariant Poisson line process is shown in Figure 8.7.

Cox line processes

Cox line processes are line processes produced by Cox processes on $\boldsymbol{C}^*$. They are characterised by their driving random measures Λ_{Cox} as in Section 5.2. Conditional on the realisation Λ of the random measure Λ_{Cox}, the point process $\Phi_{\boldsymbol{C}^*}$ in $\boldsymbol{C}^*$ is Poisson of intensity measure Λ. If the driving random measure is translation-symmetric, then so is the Cox line process. Thus a complete characterisation of stationary Cox line processes depends on the analysis of translation-symmetric random measures on $\boldsymbol{C}^*$.

It is a remarkable fact that if a translation-symmetric random measure Λ_{Cox} on $\boldsymbol{C}^*$ has locally finite second moment measure, and gives zero measure to the set of lines parallel to the cylinder axis, then it must factorise into the form

$$\Lambda_{\mathrm{Cox}}\big(\mathrm{d}(p, \alpha)\big) = \mathrm{d}p \cdot \Lambda^{\Theta}(\mathrm{d}\alpha),$$

where Λ^{Θ} is a random measure on $(0, 2\pi]$. This was observed by Davidson (1974a) for translation-symmetric random measures with second moment density. The density condition was lifted by Krickeberg (1972, 1974) using disintegration of the second moment measure.

This factorisation implies that (under suitable regularity conditions) stationary Cox line processes must be mixtures of stationary Poisson line processes; in effect the line density L_A and the rose of directions $\mathscr{R}$ are randomised. A motion-invariant Cox line process must satisfy the further condition that the random measure Λ^{Θ} on $(0, 2\pi]$ is invariant under translation modulo 2π.

The central position occupied by mixed Poisson line processes is also indicated by a class of results concerning intersections of the lines of a Cox line process. These intersections form a point process that is stationary if the line process is stationary. The intensity of the intersection process (suitably normalised) is maximised by the isotropic mixed Poisson line processes; see Davidson (1974b).

Davidson's conjecture

The problem posed by Davidson (1974a) was whether or not there existed motion-invariant line processes of locally finite second moment measure which were neither Cox nor contained parallel lines. (Note that a motion-invariant line process has either no or infinitely many pairs of parallel lines or antiparallel lines; see Davidson, 1974c.) Davidson conjectured that there were no such line processes. Indeed, the geometrical properties of $\boldsymbol{C}^*$ place strong restrictions on the characteristics of stationary line processes. Under suitable regularity conditions these restrictions imply the Cox property. However, Kallenberg (1977) showed that in general there *do* exist counterexamples to Davidson's conjecture.

Example 8.3. *A stationary line process with no parallel lines which is not Cox*
The description of this line process is best given using an alternative coordinatisation to the cylindrical parametrisation. Each line ℓ in the plane is parametrised by a pair (a, b) where $a(\ell) = \cot \alpha(\ell)$ (using $\alpha(\ell)$ as in the cylindrical representation), and $b(\ell)$ is the signed distance between the origin and the intercept of ℓ on the x_1-axis. So the representation space is a plane. This coordinatisation breaks down if ℓ is parallel to the x_1-axis. However, in this example that eventuality is of probability zero.

Translations $T_{(s,\gamma)}$ of $\mathbb{R}^2$ correspond to linear shears of the representation plane:

$$T_{(s,\gamma)}(a, b) = \big(a,\ b - s(a \sin \gamma - \cos \gamma)\big)$$

and so translation-symmetries will send a linear lattice on the representation plane into another linear lattice.

Thus the corresponding class of patterns of lines (patterns that correspond under the above planar parametrisation to lattices of points) will be left invariant under the group of translations. Kallenberg constructed a probability measure on the space of lattices which is invariant under the action of the group of linear shears and hence is translation-symmetric. This example suffers the imperfection that a lattice on (a, b)-space corresponds to a line pattern that is not locally finite (there are infinitely many lines of arbitrarily small angle γ hitting each compact set). However, this imperfection is removed by a thinning depending only on the angular parameter, for example by deleting all points of the lattice lying outside a region in (a, b)-space bounded by two lines of the form $a =$ constant. The resulting process has a finite second moment measure.

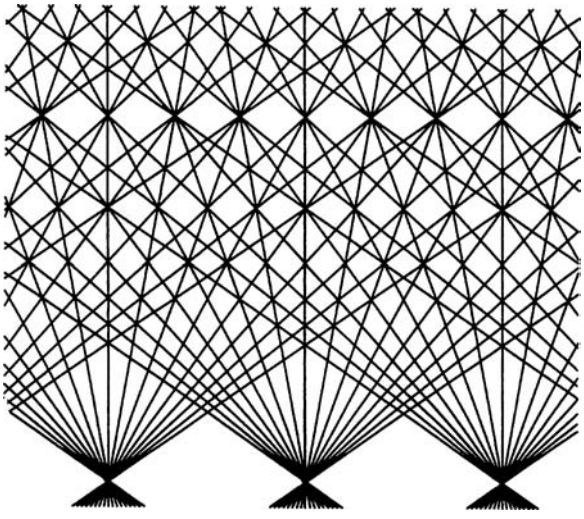

Figure 8.8 A simulated realisation of a Kallenberg lattice process. This is clearly not a Poisson line process: many intersections involve more than two lines and the pattern is very regular.

A simulation of the resulting lattice process is displayed in Figure 8.8. It is clearly not a Cox process; the lattice structure means that there is positive probability of observing more than two lines meeting at some intersections. This failure to have the *bundle-free* property follows immediately from the observation that lines meeting in a common point in the (a, b)-representation correspond exactly to collinear representing points. One might hope that if a stationary line process is both free of parallel lines and bundle-free, then it must also be Cox. Kallenberg (personal communication) has pointed out that this cannot be so; if his example is modified by independent parallel translations of the lines over random distances which are uniform on $[0, \varepsilon]$, then no bundles can occur. The modification cannot be Cox for small $\varepsilon > 0$, since this would not be compatible with the influence of the underlying lattice structure on the point representation.

The Kallenberg lattice-type line process is completely defined by a fundamental cell of the lattice in the (a, b)-space representation; Sukiasian (1987) took parabolic inversion of the lattice to construct further examples. Mecke (1979) constructed the process using only five real-valued random variables.

8.2.3 Spatial line and plane processes

The theory presented in the preceding section can be generalised. Of most practical interest are the cases of planes and lines in $\mathbb{R}^3$.

Parametric representations in $\mathbb{R}^3$

Planes in $\mathbb{R}^3$: If the planes are oriented, then they may be represented by points $(x, \boldsymbol{u})$ lying in a generalised cylinder $\mathbb{R} \times S^2$. Consider an oriented plane P. Let $\boldsymbol{u} \in S^2$ be the unit vector

normal to P defined by its orientation. Then the point on P closest to the origin is given by $x\boldsymbol{u}$ for some scalar x in $\mathbb{R}$. So the oriented plane P is parametrised by $(x, \boldsymbol{u}) \in \mathbb{R} \times S^2$. Unoriented planes are parametrised by a space obtained by identifying points $(x, \boldsymbol{u})$ and $(-x, -\boldsymbol{u})$. Away from $x = 0$ the unoriented representation space is given by $(0, \infty) \times S^2$, but there are topological complications at $x = 0$. An alternative is $\mathbb{R} \times S^2_+$, where S^2_+ consists of the points of S^2 with nonnegative x_3-coordinate. See also Baddeley and Jensen (2005, p. 92).

Lines in $\mathbb{R}^3$: For topological reasons, this case is more complicated than the cases considered until now. If the lines are oriented, then they may be represented by points $\big(x, (\boldsymbol{u}, \boldsymbol{v})\big) \in [0, \infty) \times T(S^2)$, where $T(S^2)$ is the tangent bundle to the sphere S^2, namely the collection of pairs $(\boldsymbol{u}, \boldsymbol{v})$, in which $\boldsymbol{u} \in S^2$ and $\boldsymbol{v}$ is a unit vector tangent to S^2 at $\boldsymbol{u}$. The point on the line which is closest to the origin is $(x, \boldsymbol{u})$, while the line's direction is $\boldsymbol{v}$. However, this representation behaves badly at $x = 0$, where $T(S^2)$ has to be replaced by S^2. If the lines are unoriented, then again pairs of points $\big(x, (\boldsymbol{u}, \boldsymbol{v})\big)$ and $\big(x, (\boldsymbol{u}, -\boldsymbol{v})\big)$ have to be identified. See also Baddeley and Jensen (2005, p. 95).

Again there is an alternative parametrisation, sometimes called the phase representation. Fix a reference plane, and represent each line by $\big((x, y), \boldsymbol{u}\big)$, where (x, y) is the intersection point of the line on the reference plane and $\boldsymbol{u}$ is the (three-dimensional) direction of the line. As before, this representation breaks down for lines parallel to the reference plane.

Decomposition of invariant measures

In each case of the above representations, expressions may be obtained for the general form of measures which are invariant under translations or under rigid motions of $\mathbb{R}^3$, analogous to Theorem 8.1; see for example Santaló (1976, II.12.7, Note 5) or Ambartzumian (1990).

Poisson line and plane processes

Poisson line processes and *Poisson plane processes* in space can now be defined simply as Poisson point processes on the corresponding representation spaces, with distributions determined by their intensity measures. As in the case of line processes on the plane, stationary and motion-invariant processes in space can be defined by requiring the point processes on the representation spaces to be translation-symmetric and motion-symmetric with respect to the corresponding induced symmetry groups.

In the stationary case the intensity parameters of main interest are the *area* or *surface density* S_V and the *line density* L_V, representing the mean total area of all plane pieces intersecting a unit cube and the mean total length of all line pieces intersecting a unit cube, respectively. As in the case of lines in $\mathbb{R}^2$ the intensity of the point process in the representative space coincides with S_V and L_V, respectively.

In the Poisson process case, the random number of planes and lines hitting a compact set K has a Poisson distribution. In the motion-invariant case and for convex K the corresponding mean μ_K satisfies

$$\mu_K = S_V\, \bar{b}(K) \qquad \text{for plane process,} \tag{8.13}$$

and

$$\mu_K = \frac{L_V}{4} S(K) \qquad \text{for line process,} \tag{8.14}$$

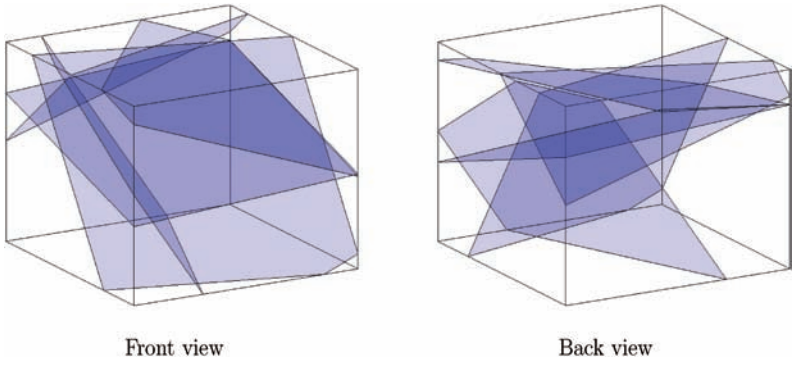

Figure 8.9 A simulated piece of a realisation of a Poisson plane process with five planes hitting a parallelepiped.

where $\overline{b}(K)$ and $S(K)$ are the average breadth and the surface area, respectively, of K. Note that there are no mutual intersections of the lines of a Poisson line process in $\mathbb{R}^3$. Figure 8.9 shows a sample of a Poisson plane process.

A hyperplane process in $\mathbb{R}^d$ generates *secondary networks* or *intersection processes* by intersections. The order-k secondary network is the process of flats each of which is the intersection of k hyperplanes from the original process. Thus under suitable regularity conditions (for example in the Poisson case) the order-d network is a point process in $\mathbb{R}^d$, while the order-1 network is the hyperplane process itself. If the hyperplane process is stationary, then so is the order-k network. Similar constructions can be given for a process of flats. The full theory for such networks is presented in Schneider and Weil (2008, Section 4.4).

Generalising work by Miles (1971a, 1974a) and Matheron (1975), Schneider and Weil (2008, Section 4.4) presented a general theory of flat processes without explicitly using representation spaces, which are, however, needed for example for simulations; see Lantuéjoul (2002).

Extending Davidson (1974b) and his treatment of the problem of maximising the intersection rate for a planar line process, Janson and Kallenberg (1981) and Mecke (1983, 1984a) used Fourier methods to produce similar results for the secondary networks of Poisson hyperplane and flat processes. Thomas (1984) applied results from convex geometry concerning the Steiner compact (see Section 8.3.1) and a generalisation of the isoperimetric inequality. This work is continued in Mecke (1986, 1988a,b, 1991) and Mecke and Thomas (1986).

Ambartzumian (1982) generalised his solution of the Buffon–Sylvester problem to the case of higher dimensions. Kallenberg (1976a, 1980, 1981) discussed generalisations to higher dimensions suggested by the Davidson problem. Kallenberg has also applied his work to the study of systems of non-interacting particles.

8.2.4 Applications of line and plane processes

Poisson and Cox line processes can be used as simple mathematical models of random systems of very long fibres of weak curvature (for example, in paper or woven materials; see Lücke and Tittel, 1993) or of trajectories of moving particles. Such models are not intended as a correct description of the global behaviour of the real structures, but can provide a useful local description. Formulae for the point process of self-intersection points and for the induced

polygons (see Section 9.5) are of interest. Kallenberg (1983b) discusses the approximation of segment processes by Cox line processes.

In another application, line processes serve as models for traffic networks; see Baccelli and Zuyev (1997), Aldous and Kendall (2008), Voss *et al.* (2009, 2010, 2011) and Kendall (2011). Fairclough and Davies (1990) use line processes in simulating the structure of fibre membranes.

Line and plane processes can be used as construction elements just as point processes are used for constructing random set models. Thus one obtains Boolean cylinder and plate models: the lines and planes are dilated to obtain cylinders or thick plates; see Section 6.6.2.

Finally, the planar Poisson line process and the Poisson plane process play an important rôle in the construction of random tessellations; see Chapter 9.

8.3 Planar fibre processes

8.3.1 Fundamentals

As mentioned above, planar fibre processes model random collections of curves in the plane $\mathbb{R}^2$. Figures 8.1 and 8.2 give examples of systems of curves or fibres that could be interpreted as samples of fibre processes. The discussion below is based on the papers of Mecke and Nagel (1980) and Mecke and Stoyan (1980a). Earlier references on fibre processes are Ambartzumian (1973, 1977), Ambartzumian and Ohanian (1975) and Cowan (1979). In these papers the fibres are usually segments and the processes are usually motion-invariant. The following treatment is more general, but theories of yet greater generality are possible.

Fibres and fibre systems

A fibre is a sufficiently smooth simple curve of finite length in the plane. More precisely, a fibre γ is a subset of $\mathbb{R}^2$ which is the image of a curve $\gamma(t) = \big(\gamma_1(t), \gamma_2(t)\big)$ such that

(i) $\gamma : [0, 1] \to \mathbb{R}^2$ is once continuously differentiable,

(ii) $|\gamma'(t)|^2 = |\gamma_1'(t)|^2 + |\gamma_2'(t)|^2 > 0$ for all t, and

(iii) the mapping γ is one-to-one, so that a fibre does not intersect itself.

Here is a deliberate ambiguity; γ also stands for the measure

$$\gamma(B) = h_1(\gamma \cap B) = \int_0^1 \mathbf{1}_B\big(\gamma(t)\big)\sqrt{\gamma_1'(t)^2 + \gamma_2'(t)^2}\,\mathrm{d}t \qquad \text{for planar Borel sets } B,$$

in which the Hausdorff measure h_1 is used, so that $h_1(\gamma \cap B)$ is simply the length of the fibre γ in the set B. Note that the *measure* γ depends only on the curve $\gamma([0, 1])$ and not on the precise representation map γ.

The definition of a fibre system is a straightforward extension of the definition of a fibre. A *fibre system* ϕ is a closed subset of $\mathbb{R}^2$ which can be represented as a union of countably many fibres $\gamma^{(i)}$, with the property that any compact set is intersected by only a finite number of the fibres, and such that distinct fibres have either nothing or only end-points in common:

$$\gamma^{(i)}\big((0, 1)\big) \cap \gamma^{(j)}\big((0, 1)\big) = \emptyset \qquad \text{whenever } i \neq j.$$

The length measure corresponding to the fibre system ϕ is then defined in terms of the measures $\gamma^{(i)}$ by

$$\phi(B) = \sum_{\gamma^{(i)} \in \phi} \gamma^{(i)}(B) \qquad \text{for Borel sets } B.$$

Despite the condition on end-points, ϕ actually may consist of intersecting curves, since fibres can end at intersection points. All the definition requires is that such curves can be dissected into a locally finite collection of fibres as above; of course, such a representation of ϕ as a union of fibres is not unique. The condition prevents fibre systems from having locally dense accumulations of self-intersection points (because of the condition of local finiteness). The local finiteness and smoothness conditions ensure that the measure ϕ is locally finite; it depends only on the closed set that is the union of all the fibres.

The family of all planar fibre systems is denoted by $\mathbb{D}$ and is endowed with a σ-algebra $\mathscr{D}$ generated by sets of the form

$$\{\phi \in \mathbb{D} : \phi(B) < x\}$$

for planar Borel sets B and positive numbers x. It can be shown that $\mathscr{D}$ is the same as the trace $\mathcal{F}_{\mathbb{D}}$ of $\mathcal{F}$ on $\mathbb{D}$, where $\mathcal{F}$ is Matheron's hitting σ-algebra for the family of all closed subsets of $\mathbb{R}^2$ as in Section 6.1.2.

Fibre processes

A (planar) *fibre process* Φ is a random variable taking values in $[\mathbb{D}, \mathscr{D}]$, that is to say, a measurable mapping from an underlying probability space $[\Omega, \mathcal{A}, \mathbf{P}]$ to $[\mathbb{D}, \mathscr{D}]$. The same symbol Φ is also used to denote the corresponding *random length measure* as well as the union set of all fibres. The theory of fibre processes is thus a special part of the theory of random measures, as well of the theory of random sets.

The *distribution* of the fibre process is the measure P generated on $[\mathbb{D}, \mathscr{D}]$ by Φ.

Stationarity and isotropy

The fibre process Φ is said to be *stationary* if it has the same distribution as the translated fibre process Φ_x for all x in $\mathbb{R}^2$. Thus

$$P(Y) = P(Y_x) \qquad \text{for all } Y \in \mathscr{D} \text{ and all } x \in \mathbb{R}^2,$$

where, as in other chapters, $Y_x = \{\phi \in \mathbb{D} : \phi_{-x} \in Y\}$. Likewise, it is *isotropic* if the distribution remains invariant under rotations about the origin. (These definitions are special cases of the general definitions for random measures or random sets.)

Intensity and the rose of directions

The *intensity measure* Λ of a fibre process is given by

$$\Lambda(B) = \mathbf{E}\big(\Phi(B)\big) = \mathbf{E}\left(\sum_{\gamma \in \Phi} h_1(\gamma \cap B)\right) \qquad \text{for Borel sets } B \text{ of } \mathbb{R}^2, \tag{8.15}$$

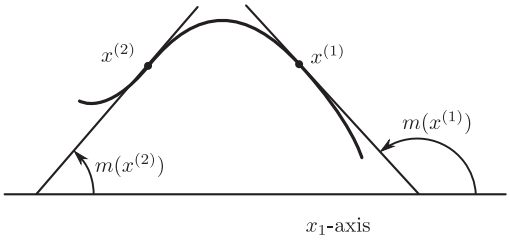

Figure 8.10 Definition of the tangent direction $m(x)$.

which is the mean length of all fibre pieces in the set B. If Φ is stationary, then invariance considerations show that there exists a constant L_A ($0 \leq L_A \leq \infty$), the *intensity* or *line density* of Φ, such that

$$\Lambda(B) = L_A \cdot \nu_2(B) \qquad \text{for Borel sets } B \text{ of } \mathbb{R}^2, \tag{8.16}$$

where ν_2 is the planar Lebesgue measure. The notation L_A stands for 'mean line length per unit area'. In fact L_A is precisely the intensity of Φ regarded as a stationary random measure. In the following L_A is assumed to be positive and finite.

The *rose of directions* arises from consideration of fibre tangents. Let $m(x)$ denote the direction of the fibre tangent at x, presuming that precisely one fibre of Φ passes through x. Then $m(x)$ is some number between 0 and π; see Figure 8.10. In the case when more than one fibre passes through x, or an end-point occurs at x, let $m(x)$ equal π; such points form a subset of h_1-measure zero by the conditions on fibre systems. Denote by $\mathcal{B}^2$ and Π the families of Borel sets of $\mathbb{R}^d$ and $(0, \pi]$, respectively, then a marked (or weighted) random measure Ψ can be defined on $\mathcal{B}^2 \times \Pi$ by

$$\Psi(B \times L) = \int_B \mathbf{1}_L\big(m(x)\big)\Phi(\mathrm{d}x) \qquad \text{for } B \in \mathcal{B}^2 \text{ and } L \in \Pi. \tag{8.17}$$

Thus $\Psi(B \times L)$ is the total length of all fibre pieces of Φ in B that have tangent directions lying in L.

If Λ_Ψ is the intensity measure of Ψ, so that

$$\Lambda_\Psi(B \times L) = \mathbf{E}\big(\Psi(B \times L)\big), \tag{8.18}$$

and if Φ is stationary, then invariance considerations dictate that Λ_Ψ can be decomposed as

$$\Lambda_\Psi(B \times L) = L_A \cdot \nu_2(B)\mathscr{R}(L), \tag{8.19}$$

where $\mathscr{R}$ is a distribution on Π, called the *rose of directions* of the fibre process Φ. Reference to Section 7.1.4 shows that this is a mark distribution. In analogy to similar constructions in the theory of point processes, $\mathscr{R}$ can be interpreted as the distribution of the direction of the tangent to a fibre at the typical fibre point. (The term 'typical fibre point' is related to the Palm distribution of the random measure associated with the fibre process; see Chapter 7.) Figure 8.2 includes an example of an empirical rose of directions.

This analogy carries further: a *Campbell theorem* also holds for stationary fibre processes, which is stated as follows.

Theorem 8.3. *Suppose Φ is a stationary fibre process with distribution P, intensity L_A and rose of directions $\mathscr{R}$. For any measurable $f : \mathbb{R}^2 \times (0, \pi] \to [0, \infty)$,*

$$\mathbf{E}\left(\int f\big(x, m(x)\big)\Phi(\mathrm{d}x)\right) = \int_{\mathbb{D}} \int_{\mathbb{R}^2} f\big(x, m(x)\big)\phi(\mathrm{d}x)P(\mathrm{d}\phi)$$
$$= L_A \int_{\mathbb{R}^2} \int_{(0,\pi]} f(x, \alpha)\, \mathscr{R}(\mathrm{d}\alpha)\, \mathrm{d}x. \tag{8.20}$$

By definition neither L_A nor $\mathscr{R}$ changes if the underlying fibre process is translated. Furthermore L_A does not vary if the fibre process is rotated; but, of course, $\mathscr{R}$ will then change. If $\boldsymbol{r}$ is an anticlockwise rotation about o through an angle θ, then the rotated fibre process has rose of directions $\boldsymbol{r}(\mathscr{R})$ where

$$\boldsymbol{r}(\mathscr{R})(L) = \mathscr{R}\big(\boldsymbol{r}^{-1}(L)\big) \qquad \text{for all Borel sets } L \text{ of } (0, \pi].$$

The inverse rotation $\boldsymbol{r}^{-1}$ is a clockwise rotation through θ.

Finite measures on $(0, \pi]$ can be represented in terms of their *Steiner compacts* S, first used for this purpose by Matheron (1975). (Schneider and Weil, 2008, use the term 'associated zonoid'.) These are centrally symmetric compact convex sets. For a stationary fibre process Φ the modified support function $s_m(S, \beta)$ of the Steiner compact S is given by

$$s_m(S, \beta) = \frac{1}{2} L_A \int_{(0,\pi]} |\sin(\alpha - \beta)| \mathscr{R}(\mathrm{d}\alpha) \qquad \text{for } 0 < \beta \leq \pi. \tag{8.21}$$

This concept aids the presentation of the important Formula (8.42). The notion of the modified support function for a symmetric convex set is described in Section 1.6. The rose of directions of the boundary ∂S of S is equal to the rose of directions $\mathscr{R}$ of Φ if rotated by $\pi/2$.

If the rose of directions $\mathscr{R}$ is the uniform distribution on $(0, \pi]$, then the resulting Steiner compact S is the ball

$$S = B\left(o, \frac{L_A}{\pi}\right). \tag{8.22}$$

By construction, the Steiner compact is homogeneous of degree -1 with respect to dilations of the process, and thus its radius, if S is a disc, has dimension length^{-1}.

The Steiner compact is an auxiliary convex body used in the study of intersections of fibre processes with lines; see Section 8.3.2. It is also a valuable tool in statistics. Two further relationships with stationary fibre processes are:

(1) if S is the Steiner compact of Φ, then $L_A = L(S)/2$, where $L(S)$ denotes the perimeter of S;

(2) if Φ_1 and Φ_2 are independent stationary fibre processes with Steiner compacts S_1 and S_2 respectively, then the Steiner compact of the union $\Phi_1 \cup \Phi_2$ is $S = S_1 \oplus S_2$.

Instead of tangent directions, fibre normals also can be considered. Sometimes it makes sense to consider the normals as directed, for example when the fibres are boundary lines of random sets and outer (outward-pointing) normals can be defined. Then one speaks about *oriented direction distributions*; see Rataj (1996).

The second moment measure and the reduced second moment measure

Moment measures for fibre processes can be defined as for general random measures. In particular the *second moment measure* $\mu^{(2)}$ of Φ is given by

$$\mu^{(2)}(B_1 \times B_2) = \mathbf{E}\big(\Phi(B_1)\Phi(B_2)\big) \qquad \text{for } B_1, B_2 \in \mathcal{B}^2. \tag{8.23}$$

In the stationary case this measure can be decomposed just as for random measures in Section 7.2.2. Given $\mu^{(2)}$ for a stationary fibre process a measure $\mathscr{K}$ can be defined on the plane by

$$\mu^{(2)}(B_1 \times B_2) = L_A^2 \int\int \mathbf{1}_{B_1}(x)\mathbf{1}_{B_2}(x+h)\,\mathrm{d}x\,\mathscr{K}(\mathrm{d}h) \qquad \text{for } B_1, B_2 \in \mathcal{B}^2. \tag{8.24}$$

This $\mathscr{K}$ is the *reduced second moment measure* of Φ. Its interpretation follows the point process case: if x is the typical fibre point of Φ, then $L_A\,\mathscr{K}(B)$ is the mean total length of all fibre pieces of Φ in B_x. This is further discussed in Stoyan (1981), Schwandtke (1988), Jensen *et al*. (1990a,b) and Zähle (1990) for the isotropic case (and also for more general, not necessarily fibrous structures) and in Beneš (1994) for the anisotropic case.

In the case of stationarity and isotropy it is sufficient to consider the *reduced second moment function* $K(r)$ given by

$$K(r) = \mathscr{K}\big(B(o,r)\big) \qquad \text{for } r \geq 0.$$

If $K(r)$ is differentiable then, just as in the point process case, one can consider the *pair correlation function* $g(r)$ given by

$$g(r) = \frac{1}{2\pi r}\frac{\mathrm{d}K(r)}{\mathrm{d}r} \qquad \text{for } r \geq 0. \tag{8.25}$$

Example 8.4. *Basic characteristics of two simple planar fibre processes*
(a) Let Φ be a motion-invariant Poisson line process of intensity L_A. Its reduced second moment function $K(r)$ is given by

$$L_A K(r) = 2r + L_A \pi r^2 \qquad \text{for } r \geq 0. \tag{8.26}$$

The pair correlation function is therefore

$$g(r) = 1 + \frac{1}{L_A \pi r} \qquad \text{for } r \geq 0. \tag{8.27}$$

To make a heuristic argument for Formula (8.26), note that $L_A K(r)$ has two components: one is the contribution from the line containing the typical point and the other is formed from the remainder of the process. Clearly the first component is $2r$. By the Slivnyak–Mecke theorem the remainder of the process has a distribution equal to that of the original process and thus it yields the contribution $L_A \nu_2\big(B(o,r)\big)$.

(b) Let Φ be a Boolean segment process as in Example 8.1 on p. 298. If the length of the typical segment has distribution function $L(x)$ with mean $\bar{l}$, then the intensity of Φ is $L_A = \lambda\,\bar{l}$, where λ is the intensity of the germ process. The reduced second moment function $K(r)$ is

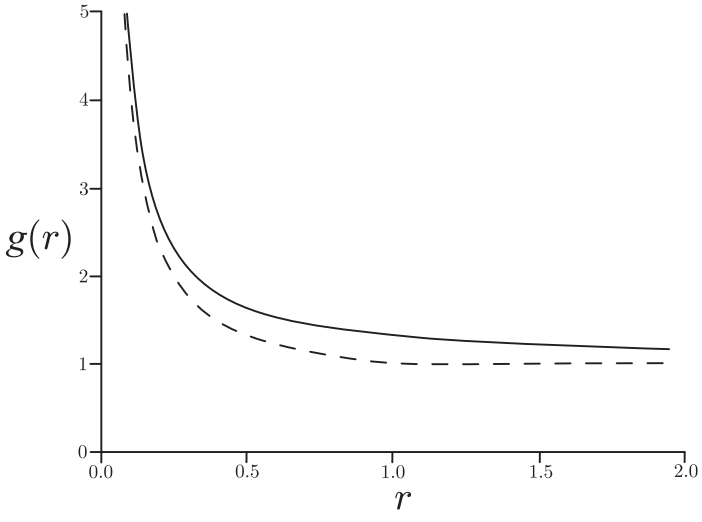

Figure 8.11 Pair correlation function $g(r)$ of a Poisson line process (—) with unit intensity and of a Boolean segment process (- - -) with segments of constant unit length and unit intensity. Note that the curve for the segment process is horizontal for $r \geq 1$.

given by

$$L_A K(r) = L_A \pi r^2 + \frac{1}{\bar{l}} \left(\int_0^r x^2 \, \mathrm{d}L(x) + \int_r^\infty (2xr - r^2) \, \mathrm{d}L(x) \right) \qquad \text{for } r \geq 0, \quad (8.28)$$

as in Stoyan (1983). Again the Slivnyak–Mecke theorem explains this; this time the second term arises from the segment on which the typical point lies. The distribution of the length of the typical segment is length-biased and the typical point lies uniformly at random on this segment.

Figure 8.11 shows the pair correlation functions for the two fibre process models in Example 8.4. As r tends to infinity, they tend to 1, but for $r \downarrow 0$ they diverge to infinity. This divergence is typical for fibre processes. It is explained by noting that even in very small discs about the typical fibre point there must still be pieces of at least one fibre. Thus $\mathrm{d}K/\mathrm{d}r$ does not become small for small r.

The corresponding quantity for point processes uses the second-order *factorial* moment measure, deleting the typical point itself. A similar approach for fibre processes using, for example, $K_0(r) = K(r) - 2r/L_A$ does not in general dispose of the infinity at zero. Note also that even in the point process case there are examples with pair correlation function having pole at zero; see the discussion in Stoyan (1994).

Weiss *et al.* (2010) gave formulae for the pair correlation and K-functions of the systems of edges of some motion-invariant tessellations, the so-called STIT tessellations; see p. 354. They showed that these second-order characteristics are identical to these of a closely related Boolean segment process.

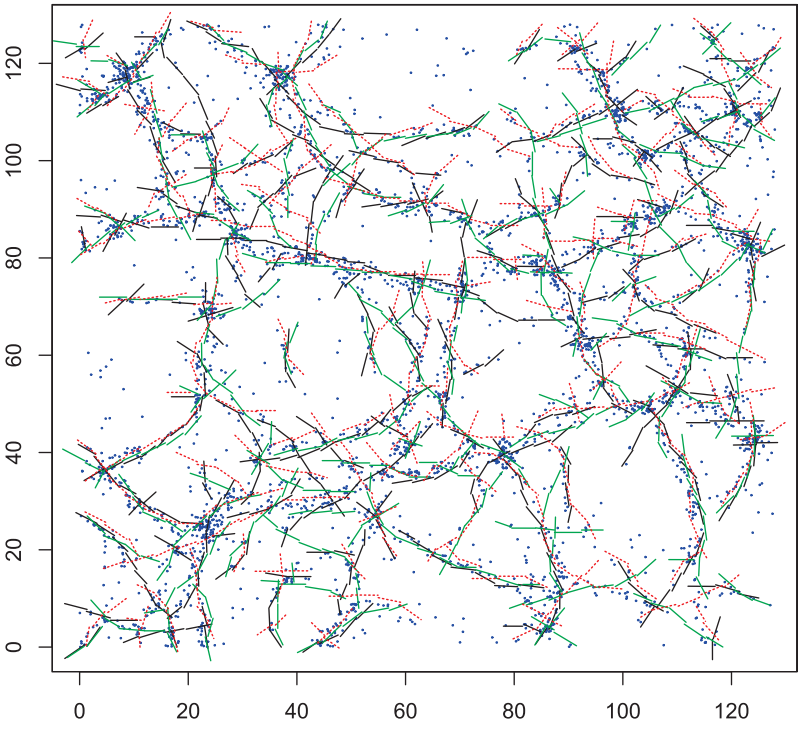

Figure 8.12 Three (—, — and ---), superposed, samples of the Candy model, simulated by a Metropolis–Hastings algorithm with three different sets of model parameters. The aim is to describe filaments of galaxies, which are shown as points, and the unit of measurement is h^{-1} Mpc. The three sets of parameters give almost equally good results. See Stoica *et al.* (2005). Courtesy of R. Stoica.

Candy model

The paper of van Lieshout and Stoica (2003) studies the properties of the so-called *Candy model*. (Its name comes from dubbing a segment as 'candy'.) This is a (planar) finite fibre process with a Gibbs distribution, where the energy function discourages free and singly connected segments as well as sharp crossings and disagreements in orientation of close segments. This model has its origin in statistics for networks of rivers and roads. Figure 8.12 shows simulated samples in an astronomical study.

Still more complicated Gibbs fibre processes have been studied in the context of polymers, based on theories of Flory (e.g. Flory, 1969) and de Gennes (e.g. de Gennes, 1979); see den Hollander (2009) and Caravenna *et al.* (2011). Hill *et al.* (2012) used rather degenerate fibre processes as part of an MCMC algorithm to reconstruct curvilinear structures from point patterns.

Undirected line processes regarded as fibre processes

In Example 8.4 above a Poisson line process is considered as a particular kind of fibre process. This is correct since every line can be considered as a union of line segments, which can be

considered as fibres. The union of all lines can also be considered as a random set, and finally a random measure can be associated with the lines, namely, the line length measure as on p. 307 and the line density L_A considered on p. 308 is the line density in the fibre process interpretation.

If the direction $\alpha(l)$ of each line l in a line process Φ is taken into account, then a marked random measure can be introduced. The direction of an undirected line lies in $(0, \pi]$, so one can define

$$\Psi(B \times L) = \sum_{\{l \in \Phi:\, \alpha(l) \in L\}} h_1(B \cap l) \qquad \text{for } B \in \mathcal{B}^2 \text{ and } L \in \Pi, \tag{8.29}$$

where $\mathcal{B}^2$ and Π are the families of Borel sets of $\mathbb{R}^2$ and $(0, \pi]$, respectively. In the stationary case the intensity measure Λ of Ψ factorises as

$$\Lambda(B \times L) = L_A \cdot \nu_2(B)\, \mathscr{R}(L) \qquad \text{for } B \in \mathcal{B}^2 \text{ and } L \in \Pi, \tag{8.30}$$

where $\mathscr{R}$ is a probability measure on $(0, \pi]$, the rose of directions. This rose has a double interpretation: as the rose of directions in the fibre-process sense and as the distribution of the direction of the typical line l of Φ.

Contact distribution functions

Up to this point the exposition has concentrated on random-measure characteristics of fibre processes. However, random-set characteristics are also of interest. Of course, area fraction p and covariance $C(r)$ are simply equal to zero. In contrast, the contact distributions make sense and give distributional information that L_A and the rose of directions cannot give.

In the case of a motion-invariant Poisson line process with line density L_A, the contact distribution function $H_B(r)$ with respect to a convex compact structuring element B is

$$H_B(r) = 1 - \exp\left(-\frac{L_A}{\pi}\, L(B)\, r\right) \qquad \text{for } r \geq 0. \tag{8.31}$$

In particular, the spherical contact distribution function is

$$H_s(r) = 1 - \exp(-2L_A r) \qquad \text{for } r \geq 0. \tag{8.32}$$

For a Boolean segment process as in Example 8.4 above it is

$$H_s(r) = 1 - \exp\bigl(-\lambda r(2\bar{l} + \pi r)\bigr) \qquad \text{for } r \geq 0. \tag{8.33}$$

These formulae simply follow from the fact that the random number of lines or segments hitting $B(o, r)$ has a Poisson distribution, and $H_s(r)$ is just the complement of probability that no hit happens.

Last and Schassberger (2000) studied the Palm inversion formula of the fibre (surface) process Φ of the edges (cell boundaries) of a general stationary tessellation in $\mathbb{R}^2$ (in $\mathbb{R}^d$), associated with a random vector field that is smooth in $\mathbb{R}^d \setminus \Phi$ but discontinuous on Φ. A formula for certain generalised contact distribution functions of Φ was obtained.

8.3.2 Intersections of fibre processes

Intersections with lines

Important methods of measurement for fibre processes use enumeration of intersections with test systems of lines, circles, or other curves. Therefore it is helpful to derive formulae for the random point patterns which arise from such intersections and, more generally, from the intersections of fibre processes with other fibre processes.

Let Φ be a stationary fibre process with distribution P, intensity L_A, and rose of directions $\mathscr{R}$ satisfying $\mathscr{R}(\{\pi\}) < 1$. Consider the intersection of Φ with a fixed line e. To be definite e is taken to be the x_1-axis.

The process $\Phi \cap e$ is a point process on e and is marked (weighted) by the angles of intersection. This marked point process $\Psi = \{[y_n; m(y_n)]\}$ was first considered by Davidson (1974b), and later discussed in Ambartzumian (1974a, 1977, 1982) and Mecke and Stoyan (1980a). The rose $\mathscr{R}$ can be recovered from the distribution of Ψ, as can L_A if $\mathscr{R}(\{\pi\}) = 0$. As will be shown below, if the fibre process Φ is not just stationary but also isotropic, and if no fibres contain linear segments, then the reduced second moment function $K(r)$ can be determined from knowledge of the distribution of Ψ.

Let P_L be the intensity of Ψ and H its mark distribution on $(0, \pi]$. The mark distribution of Ψ is the distribution of the intersection angle at the typical point of the intersection point process $\Phi \cap e$.

The following formula connects the characteristics of Φ and Ψ:

$$P_L \int_{\mathbb{R}} \int_{(0,\pi]} h(z, \alpha) H(\mathrm{d}\alpha)\, \mathrm{d}z = L_A \int_{\mathbb{R}} \int_{(0,\pi]} h(z, \alpha) \sin\alpha\, \mathscr{R}(\mathrm{d}\alpha)\, \mathrm{d}z, \tag{8.34}$$

where h is any nonnegative and measurable function on $\mathbb{R} \times (0, \pi]$. Formula (8.34) can be proved as follows.

Proof. Let ϕ be any fibre system, and let w be any nonnegative measurable function on $\mathbb{R}^2 \times (0, \pi]$. Furthermore, let $m(x)$ be the direction of the fibre tangent of Φ at x. Simple geometry shows that

$$\int_{\mathbb{R}^2} w\big(x, m(x)\big) \sin m(x) \phi(\mathrm{d}x) = \int_{\mathbb{R}} \sum_{x_1:(x_1, x_2)\in\phi} w\big((x_1, x_2), m(x_1, x_2)\big)\, \mathrm{d}x_2. \tag{8.35}$$

If g is a nonnegative measurable function with $\int_{\mathbb{R}} g(z)\, \mathrm{d}z = 1$, then the Campbell theorem (8.20) can be employed on Φ for

$$f(x, \alpha) = h(x_1, \alpha)\, g(x_2) \sin\alpha,$$

leading to

$$\mathbf{E}\left(\int_{\mathbb{R}^2} h\big(x_1, m(x)\big) g(x_2) \sin m(x) \Phi(\mathrm{d}x) \right) = L_A \int_{\mathbb{R}^2} \int_{(0,\pi]} h(x_1, \alpha) g(x_2) \sin\alpha\, \mathscr{R}(\mathrm{d}\alpha)\, \mathrm{d}x.$$

The right-hand side equals

$$L_A \int_{\mathbb{R}} \int_{(0.\pi]} h(z, \alpha) \sin\alpha\, \mathscr{R}(\mathrm{d}\alpha)\, \mathrm{d}z,$$

and by Formula (8.35) for $w\big(x_1, x_2, m(x)\big) = h\big(x_1, m(x)\big)g(x_2)$ and stationarity, the left-hand side becomes

$$\begin{aligned}
\mathbf{E}\left(\int_{\mathbb{R}} \sum_{x_1:(x_1,\,x_2)\in\Phi} h\big(x_1, m(x)\big)\, g(x_2)\,\mathrm{d}x_2\right) &= \int_{\mathbb{D}}\int_{\mathbb{R}} \sum_{x_1:(x_1,\,x_2)\in\phi} h\big(x_1, m(x)\big)\, g(x_2)\,\mathrm{d}x_2 P(\mathrm{d}\phi)\\
&= \int_{\mathbb{R}}\int_{\mathbb{D}} \sum_{x_1:(x_1,\,x_2)\in\phi-(0,\,x_2)} h\big(x_1, m(x_1,0)\big) P(\mathrm{d}\phi)\, g(x_2)\,\mathrm{d}x_2\\
&= \int_{\mathbb{D}} \sum_{x_1:(x_1,\,0)\in\phi} h\big(x_1, m(x_1,0)\big) P(\mathrm{d}\phi)\\
&= \mathbf{E}\left(\sum_{[y;\,m(y)]\in\Psi} h\big(y, m(y)\big)\right).
\end{aligned}$$

The proof is completed by applying the Campbell theorem (4.20) for the marked point process Ψ to this last formula. □

From (8.34) one can derive some important formulae, relating characteristics of Φ to those of Ψ. For example, the intensity of Ψ is related to the intensity and rose of directions of Φ by

$$P_L = L_A \int_{(0,\pi]} \sin\alpha\, \mathscr{R}(\mathrm{d}\alpha), \tag{8.36}$$

as can be seen by putting $h(z,\alpha) = \mathbf{1}_{[0,1]}(z)$.

If $h(z,\alpha) = \mathbf{1}_{[0,1]}(z)\mathbf{1}_{(0,\beta]}(\alpha)$ for some β in $(0,\pi]$, then a more refined relation is obtained that uses also the mark distribution H

$$P_L H\big((0,\beta]\big) = L_A \int_{(0,\beta]} \sin\alpha\, \mathscr{R}(\mathrm{d}\alpha) \qquad \text{for } 0 < \beta \le \pi. \tag{8.37}$$

It follows that the orientation distribution function $F_H(\beta)$ for H is given by

$$F_H(\beta) = H\big((0,\beta]\big) = \frac{\int_{(0,\beta]} \sin\alpha\, \mathscr{R}(\mathrm{d}\alpha)}{\int_{(0,\pi]} \sin\alpha\, \mathscr{R}(\mathrm{d}\alpha)} \qquad \text{for } 0 < \beta \le \pi.$$

When $\mathscr{R}$ is the uniform distribution on $(0,\pi]$, as in the case of isotropy, then

$$P_L = \frac{2}{\pi} L_A \tag{8.38}$$

and

$$F_H(\beta) = \frac{1}{2}(1 - \cos\beta) \qquad \text{for } 0 < \beta \le \pi, \tag{8.39}$$

with the corresponding density function

$$f_H(\beta) = \frac{1}{2}\sin\beta \qquad \text{for } 0 < \beta \leq \pi.$$

This density also arises in the case of intersection with curves; see Morton (1966).

Let $\mathscr{R}(\{\pi\}) = 0$ so that a typical point on a fibre has fibre tangent almost surely not parallel to the sampling line e. Then the characteristics of Φ can be expressed in terms of those of Ψ:

$$\mathscr{R}\big((0, \beta]\big) = \frac{P_L}{L_A}\int_{(0,\beta]} (\sin\alpha)^{-1} H(\mathrm{d}\alpha) \tag{8.40}$$

and

$$L_A = P_L \int_{(0,\pi]} (\sin\alpha)^{-1} H(\mathrm{d}\alpha). \tag{8.41}$$

A further formula for $\mathscr{R}$ involves the so-called *rose of intersections* $P_L(\beta)$, which is the intensity of the point process of intersection points of Φ with a sampling line at angle β to e. Up to a factor this is the same as the modified support function of the Steiner compact S related to $L_A\mathscr{R}$, as described above in Section 8.3.1.

Consider the point process of intersections of Φ with a straight line forming the angle β with the reference axis. The fibre system rotated by $\boldsymbol{r}$ has rose of directions $\boldsymbol{r}(\mathscr{R})$ as explained in Section 8.3.1. Thus if $\boldsymbol{r}$ rotates through an angle $-\beta$ sending the intersection line to e, then Formula (8.36) can be applied to the rotated fibre process. This shows that the point process of intersection points has intensity

$$P_L(\beta) = L_A \int_{(0,\pi]} |\sin(\alpha - \beta)|\, \mathscr{R}(\mathrm{d}\alpha) = L_A \int_0^{\pi} |\sin(\alpha - \beta)|\, f_{\mathscr{R}}(\mathrm{d}\alpha). \tag{8.42}$$

This formula was first given by Hilliard (1962). Here one speaks about the *sine transform* (of the density function $f_{\mathscr{R}}(\alpha)$ corresponding to the rose of directions).

Formulae (8.21) and (8.42) together yield

$$P_L(\beta) = 2s_m(S, \beta) \qquad \text{for } 0 < \beta \leq \pi. \tag{8.43}$$

Hence there is a direct connection between the rose of intersections and the modified support function $s_m(S, \beta)$ of the Steiner compact S of Φ. If $\mathscr{R}$ has a continuous density function $f_{\mathscr{R}}(\beta)$, then Formula (8.42) can be differentiated to show

$$\frac{\mathrm{d}^2 P_L(\beta)}{\mathrm{d}\beta^2} + P_L(\beta) = 2L_A f_{\mathscr{R}}(\beta) \qquad \text{for } 0 < \beta \leq \pi. \tag{8.44}$$

The case where a density does not exist is considered in Berg (1969) and Mecke (1981a). In principle the formula allows for estimation of $f_{\mathscr{R}}(\beta)$ if the rose of intersections $P_L(\beta)$ is calculated empirically. In practice one must deal with the serious problems of numerical differentiation of $P_L(\beta)$.

A simple example of an anisotropic fibre process is the 'pressed' fibre process discussed in Stoyan *et al.* (1980). This is produced from an isotropic fibre process by the 'pressing' mapping

$$p_c : (x_1,\ x_2) \to (x_1,\ c \cdot x_2) \qquad \text{for some } c \text{ with } 0 < c < 1.$$

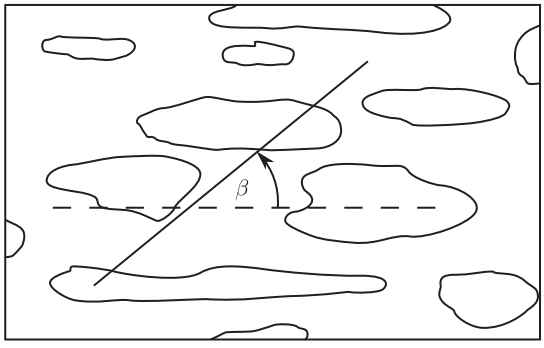

Figure 8.13 A sample of a pressed fibre process together with a 40° measurement line.

Characteristics of the pressed fibre process can be expressed in terms of the original isotropic fibre process. For example, its intensity satisfies in good accuracy and independently of c

$$L_A \approx \frac{\pi}{2} P_L(\beta) \qquad \text{for } \beta = 40^\circ, \tag{8.45}$$

see Figure 8.13. This result is obtained by numerical calculation of the elliptic integral which appears in the formula for $P_L(\beta)$ for the pressed fibre process.

For a motion-invariant fibre process Φ, the reduced second moment function $K(r)$ can be determined in terms of the marked intersection point process Ψ together with certain additional marks. If $[y; m(y)]$ belongs to Ψ, then the additional mark on y required is

$$s_r(y) = L(y) + 2\pi \sum_{\substack{(x_1,\,0)\in\Phi,\\ y\le x_1\le y+r}} \frac{x_1 - y}{\sin\alpha(x_1, 0)},$$

where $\alpha(x_1, 0)$ is the intersection angle between the fibre at $(x_1, 0)$ and the x_1-axis (so $0 < \alpha(x_1, 0) \le \pi$), and $L(y)$ is the total length of all straight line pieces of fibres lying on lines radial to $(y, 0)$ within the ball $B\big((y, 0), r\big)$.

Note that if Φ has no straight line pieces of fibre, then $s_r(y)$ is determined entirely by the information contained within the marked point process Ψ. However, the additional information represented by the lengths $L(y)$ is required if there are straight pieces of fibre in Φ.

Consider the new marked point process $\{[y; m(y), s_r(y)]\}$ and let $\mathscr{I}$ be the joint mark distribution of the mark pair $\big(m(y), s_r(y)\big)$. Then it holds that

$$L_A\, K(r) = \frac{2}{\pi} \int_{[0,\infty)} \int_{(0,\pi]} \frac{s}{\sin\alpha} \mathscr{I}\big(\mathrm{d}(\alpha, s)\big) \qquad \text{for } r \ge 0, \tag{8.46}$$

as shown by Stoyan (1981). Ambartzumian (1981) studied the particular case of segment processes and gave formulae for the product density, which agrees with the pair correlation function up to a factor L_A^2. Formula (8.46) is refined and generalised in Schwandtke (1988). The general theory behind these results is presented in Jensen *et al.* (1990a,b) and Zähle (1990), where also higher-dimensional analogues are considered.

The properties of intersection of fibres processes having segments, triangles, and circles as fibres are studied in Ohanian (1978) and Sukiasian (1978, 1980).

Intersections with fibre systems

Suppose that Φ is a stationary fibre process of intensity L_A and rose of directions $\mathscr{R}$, and that ψ is a nonrandom fibre system with finite total length l. Mecke (1981a) and Ohser (1981) studied the intersection process $\Phi \cap \psi$. This intersection is a point process with only a finite number of points because ψ has finite total length. The fibre system ψ controls the basic characteristics of $\Phi \cap \psi$ by means of two functional parameters:

(a) the angle distribution η_ψ, a probability measure on $(0, \pi]$ given by

$$\eta_\psi(L) = \frac{h_1(\{x \in \psi : m_\psi(x) \in A\})}{l} \qquad \text{for Borel sets } L \text{ of } (0, \pi], \tag{8.47}$$

where $m_\psi(x)$ is the ψ-fibre tangent angle at x;

(b) the total length $\varrho_\psi(\beta)$ (counted by multiplicity) of the projection of ψ in the direction β, given by

$$\varrho_\psi(\beta) = \int_{l_\beta^\perp} \#\{\psi \cap (l_\beta - y)\}\, \mathrm{d}y \qquad \text{for } 0 < \beta \leq \pi,$$

where l_β is a line of direction β and $l_\beta^\perp$ is a line perpendicular to l_β.

Here are two examples of these characteristics for particular ψ:

(1) if ψ is a circle of radius R, then η_ψ is uniform on $(0, \pi]$ and $\varrho_\psi(\beta) = 2l/\pi$ for all $\beta \in (0, \pi]$ (note that $l = 2\pi R$);

(2) if ψ is the union of two segments of equal lengths $l/2$ that make angles α and $\alpha + \pi/2$ with the x_1-axis respectively, then η_ψ is the obvious two-point distribution on $\{\alpha, \alpha + \pi/2\}$ and

$$\varrho_\psi(\beta) = \frac{l}{2}\,(|\sin(\beta - \alpha)| + |\cos(\beta - \alpha)|) \qquad \text{for } 0 < \beta \leq \pi.$$

The mean number of points $\overline{N}_\psi$ of $\Phi \cap \psi$ satisfies

$$\overline{N}_\psi = L_A\, l \int_{(0,\pi]} \int_{(0,\pi]} |\sin(\alpha - \beta)|\, \mathscr{R}(\mathrm{d}\alpha)\eta_\psi(\mathrm{d}\beta). \tag{8.48}$$

If ψ is a circle of radius R, then (independently of $\mathscr{R}$)

$$\overline{N}_\psi = 4RL_A. \tag{8.49}$$

If $\overline{N}_\psi(L)$ denotes the mean number of points in $\Phi \cap \psi$ for which the Φ-fibre direction is in the Borel set L of $(0, \pi]$, then

$$H_\psi(L) = \frac{\overline{N}_\psi(L)}{\overline{N}_\psi} \qquad \text{for all } L \in \Pi$$

defines a distribution on $(0, \pi]$ which can be interpreted as the angle distribution for the intersections. It satisfies

$$\overline{N}_\psi H_\psi(L) = L_A \int_L \varrho_\psi(\alpha) \mathscr{R}(\mathrm{d}\alpha), \tag{8.50}$$

and if, in particular, ψ is a circle, then

$$H_\psi = \mathscr{R}. \tag{8.51}$$

Intersection of two fibre processes

Let Φ_1 and Φ_2 be two independent stationary fibre processes of characteristics $L_{A,i}$ and $\mathscr{R}_i$ for $i = 1$ and 2. The intersection $\Phi_1 \cap \Phi_2$ is a stationary point process, the intensity of which is denoted by λ. Then

$$\lambda = L_{A,1} L_{A,2} \int_{(0,\pi]} \int_{(0,\pi]} |\sin(\alpha_1 - \alpha_2)| \mathscr{R}_1(\mathrm{d}\alpha_1) \mathscr{R}_2(\mathrm{d}\alpha_2). \tag{8.52}$$

If either of the roses $\mathscr{R}_2$ or $\mathscr{R}_2$ is actually uniform on $(0, \pi]$ (and this will occur for example if either of the Φ_i is isotropic), then Formula (8.52) simplifies to

$$\lambda = \frac{2}{\pi} L_{A,1} L_{A,2}. \tag{8.53}$$

A formula for the reduced second moment measure of $\Phi_1 \cap \Phi_2$ is given in Hanisch (1985).

8.3.3 Basic statistical methods for planar fibre processes

General

In general, estimation of basic characteristics of fibre processes follows the same path as the case of point processes. However, there is an important difference in the process of model fitting as there is no fibre process model holding a central position analogous to that of the Poisson point process.

There seem to be only a few references on statistics for particular fibre process *models*. Fellous *et al.* (1978) and Rasson and Hermans (1988) wrote on statistics for line processes. Laslett (1982a,b), Gill (1994), van de Laan (1995), Wijers (1995) and van Zwet (2004) studied the estimation of segment length distributions for segment processes.

In this section estimation procedures are discussed for the basic characteristics L_A, $\mathscr{R}$ and K. In every case it is assumed that the data arise as a sample of the fibre process Φ observed in a compact window of observation W. It can be useful to approximate the observed image by systems of segments; see Scheidegger (1979) and Stoyan and Stoyan (1983). In an analysis without the aid of an image analyser this can be helpful, as it simplifies length and angle measurements. More generally it may serve as a useful smoothing procedure when the fibres are irregular.

Estimation of L_A

The most natural unbiased estimator of L_A is

$$\hat{L}_A = \frac{\Phi(W)}{\nu_2(W)}, \tag{8.54}$$

where $\Phi(W)$ is the total length of all fibre pieces in W, which in many situations can be measured by an image analyser. Otherwise, intersections with sampling lines or circles can be used and then Formulae (8.38) and (8.49) be applied. If Φ is motion-invariant, an unbiased estimator is given by

$$\hat{L}_A^{\text{segment}} = \frac{\pi \cdot \#\{T \cap \Phi\}}{2h_1(T)}, \tag{8.55}$$

where T is a test system of segments (such as an array of parallel segments) in W of total length $h_1(T)$ and $\#\{\mathrm{A}\}$ denotes the number of points in A. In the general stationary case a test system C composed of n circles of fixed radius R can be used. Formula (8.49) ensures that an unbiased estimator for L_A is

$$\hat{L}_A^{\text{circle}} = \frac{\#\{C \cap \Phi\}}{4nR}. \tag{8.56}$$

The application of these estimators is demonstrated in Example 8.6 on p. 341. Rancoita *et al.* (2011) describe a way practically realise this method. Beneš *et al.* (1994) and Beneš and Rataj (2004, pp. 61–92) propose further estimators of L_A in the anisotropic case and give their estimation variances and other properties.

Lauschmann and Mrkvička (2009) study two regression-based methods of individual perimeter measurement for systems of closed planar curves. Ambrosio *et al.* (2009) show that the intensity can be approximated by a multiple of the volume fraction of the dilated set $\Phi_{\oplus r}$ for small r.

Estimation of the rose of directions $\mathscr{R}$

There are three main approaches for estimating $\mathscr{R}$ or the corresponding density function $f_{\mathscr{R}}(\alpha)$, which can be systematised according to the data used. The reader should note that estimation of $\mathscr{R}$ based on sections and stereological ideas (as in the first method below) is an ill-posed problem of a difficulty similar to that of Wicksell's corpuscle problem (described in Section 10.4.2). As there, a *two-step method* is recommended: determine first by nonparametric methods a reasonable type of distribution and then apply parametric methods to data that can be measured in high precision. Starting from a formula for $f_{\mathscr{R}}(\beta)$ by means of (8.42), a formula for $P_L(\beta)$ is derived and then the parameters of the latter are estimated.

Rose of intersection

Smoothing methods are used in Marriott (1971) (cardioidal approximation of either $P_L(\beta)$ or $\mathscr{R}$), Serra (1975) (elliptic approximation of $P_L(\beta)$) and Louis *et al.* (2011) (using mollifiers to invert the cosine transform, which is equivalent to the sine transform in (8.42)).

Hilliard (1962) and Kanatani (1984) used Fourier methods. They compared Fourier coefficients of the two roses $P_L(\beta)$ and $\mathscr{R}$. Beneš and Gokhale (2000) showed that the obtained

estimators do not have good statistical properties; see also the cautionary remark given in Hilliard and Lawson (2003, footnote on p. 143).

Methods based on the Steiner compact S are applied in Rataj and Saxl (1989) for planar fibre processes (see also Beneš and Rataj, 2004, pp. 143–52). The first step is the construction of a polygonal estimator $\hat{S}$ of S starting from values of the rose of intersections $P_L(\beta)$ and using Formula (8.43). Then the rose of directions of the boundary $\partial\hat{S}$ of $\hat{S}$, which can be easily obtained because of the polygonal shape, is an estimator of $\mathscr{R}$. The graphical construction of $\hat{S}$ can be replaced by an analytical one; see Beneš and Gokhale (2000).

In particular, for the Poisson line process, Kiderlen (2001) proposed a maximum likelihood estimator, whose optimisation procedure can be implemented by the EM algorithm, whilst Prokešová (2003) suggested a Bayesian approach, where MCMC can be used to approximate the posterior distribution. Both of these methods were shown to yield consistent estimators of $\mathscr{R}$, even when applied to more general stationary fibre processes.

Angle-marked section process

The intersection $\Phi \cap T$ is analysed for T being a test system of circles of radius R lying in the observation window W. If $m(x)$ is the direction of the fibre tangent at x, then

$$\hat{\mathscr{R}}\big((\alpha_1, \alpha_2]\big) = \frac{1}{\#(\Phi \cap T)} \sum_{x \in \Phi \cap T} \mathbf{1}_{(\alpha_1,\alpha_2]}\big(m(x)\big) \tag{8.57}$$

is a ratio-unbiased estimator of $\mathscr{R}\big((\alpha_1, \alpha_2]\big)$; see Ohser (1981). This is because the angles at the intersection points form a sample from a population of angles of distribution $\mathscr{R}$.

Grey-tone images

When only a degraded grey-tone image of the fibre process is available, the rose of intersections $P_L(\beta)$ cannot be estimated directly. Kärkkäinen *et al.* (2001) suggest approximating its values through evaluating the intersection intensity for a given test line by grey-tone values along the line using a scaled variogram. They assume a parametric model for the rose of directions. Altendorf and Jeulin (2009) and Wirjadi *et al.* (2009) completely avoid the use of test lines.

In parametric statistics, the von Mises distribution for the planar case and the von Mises–Fisher distribution for the spatial case (see Fisher *et al.*, 1987) may be the first choice. For other parametric families, see Mardia and Jupp (2000), Jammalamadaka and SenGupta (2001), León *et al.* (2006) and Oualkacha and Rivest (2009).

Estimation of the reduced second moment function $K(r)$ and the pair correlation function

The estimation of $K(r)$ is a rather complicated matter. Various methods will be sketched. In the following Φ is always assumed to be motion-invariant; for the anisotropic case see Beneš (1994) and Weiss and Nagel (1994).

A first approach uses intersections with test systems. Let T be a system of parallel lines in a distance larger than the expected range of correlation, that is, larger than the value r_0 that it is expected that $g(r) = 1$ for all $r \geq r_0$. A simple approximation, which can give acceptable results for values of r not too small, can be obtained by assuming that the fibre-line intersection angles are independent. Then $g(r)$ and the pair correlation function of the one-dimensional

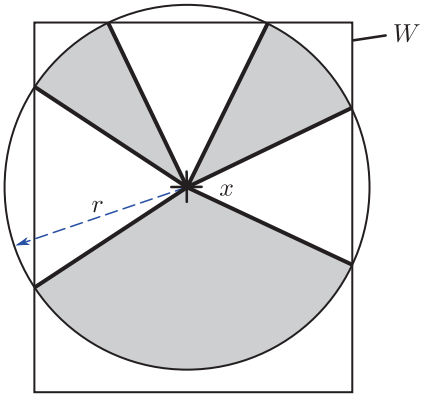

Figure 8.14 From the centre x, draw lines to the intersections between the circle $\partial B(x, r)$ and W. The set $S(x, r, W)$ is the union of the (shaded) sectors corresponding to arcs lying in W.

point process of intersection points are nearly equal, and so estimators of the latter lead to estimators of the former.

A more sophisticated method also starts with the points of $\Phi \cap T$. Formula (8.90) below provides the unbiased estimator $\hat{l}(r)$ of $L_A K(r)$

$$\hat{l}(r) = \frac{\mathbf{1}}{\#\{\Phi \cap T\}} \sum_{x \in \Phi \cap T} k(x, r) \Phi\big(S(x, r, W)\big), \tag{8.58}$$

where $S(x, r, W)$ is sketched in Figure 8.14 and $k(x, r) = 2\pi/\alpha_{x,r}$, in which $\alpha_{x,r}$ is the sum of all angles of the arcs in $\partial B(x, r) \cap W$. This estimator is based on a 'weighting' of the fibre points x by the total length $S_r(x)$ of all fibre pieces within the disc $B(x, r)$. Here fibre length measurement is necessary.

The perhaps most elegant approach is the Cox-process approach, probably first used by Hanisch (1985). For a simple example of this idea, consider first a line process. On each line, independently of the others, generate a Poisson point process with some intensity λ. The union of all these points is a sample of a Cox process with driving measure $\lambda\Phi$. By Formula (5.33) the K-function of the Cox point process coincides with the K-function of the line process, and so estimation of one yields the other. The same is true for the pair correlation functions.

The case of a process of general fibres can be treated analogously. This method can be easily realised with the help of an image analyser. If the fibre pixels are black and the rest white, then sample randomly from the black pixels and estimate the K-function or the pair correlation function for the point pattern resulting from the sample.

8.4 Spatial fibre processes

The definitions of spatial line and fibre processes follow the pattern of their planar counterparts, with occasional extra complexities; see Mecke and Nagel (1980) and Nagel (1983). This section is restricted to some brief remarks on stationary fibre processes.

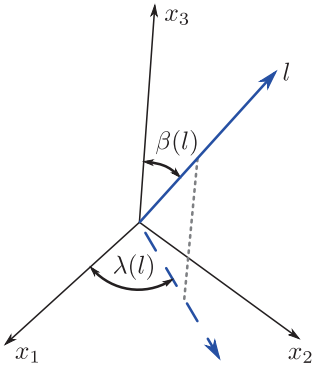

Figure 8.15 A diagram to illustrate the system of spherical polar coordinates.

As with planar fibre processes, so in this case the *intensity* L_V of a stationary spatial fibre process Φ is the mean fibre length per unit volume, and

$$L_V \nu_3(B) = \mathbf{E}\big(\Phi(B)\big) \qquad \text{for all Borel sets } B \text{ of } \mathbb{R}^3. \tag{8.59}$$

The *rose of directions* $\mathscr{R}$ is now defined as a distribution on the space $\mathbb{L}$ of all straight lines through the origin; $\mathbb{L}$ is actually the projective plane $\mathbb{RP}^2$. The corresponding Borel σ-algebra $\mathcal{L}$ is the system of all spatial Borel sets that are unions of lines through o. The quantity $\mathscr{R}(A)$ is defined by

$$L_V \nu_3(B)\mathscr{R}(A) = \mathbf{E}\left(\int_B \mathbf{1}_A\big(l(x)\big)\Phi(\mathrm{d}x)\right) \qquad \text{for } A \in \mathcal{L}, \tag{8.60}$$

where $l(x)$ is the fibre tangent line through x.

If Φ is isotropic, then $\mathscr{R}$ is the rotation-invariant, or uniform, probability distribution U_1 on $\mathbb{L}$. To describe this distribution more explicitly, introduce a coordinate system on $\mathbb{L}$. A line l in $\mathbb{L}$ makes an angle $\beta(l)$ with the x_3-axis, the *azimuthal angle*; and the projection of $l \cap \{x_3 > 0\}$ onto the plane $x_3 = 0$ makes an angle $\lambda(l)$ with the x_1-axis, the *geographical longitude*, see Figure 8.15. These angles lie in the regions

$$0 \le \beta(l) \le \frac{\pi}{2} \qquad \text{and} \qquad -\pi \le \lambda(l) \le \pi,$$

although if $\beta(l) = \pi/2$, then $\big(\beta(l), \lambda(l)\big)$ and $\big(\beta(l), \pi - \lambda(l)\big)$ refer to the same line. (This kind of duplication is inescapable, when a projective plane is coordinatised.) Under this coordinate system the measure U_1 can be expressed as

$$U_1\big(\mathrm{d}(\beta, \lambda)\big) = \frac{\sin\beta\,\mathrm{d}\beta\,\mathrm{d}\lambda}{2\pi}. \tag{8.61}$$

The intersection of a spatial fibre process with a plane e (consider for simplicity this plane e to be the plane $x_3 = 0$) generates a point process on e. A point x of this point process can be marked with the fibre tangent line $l(x)$ through x in $\mathbb{L}$. Thus the intersection generates a stationary marked point process

$$\Psi = \{[x; l(x)]\}.$$

If P_A is the intensity of Ψ and Θ its mark distribution, then by analogy with Formula (8.34), these can be connected to the characteristics of the fibre process using a formula of Mecke and Nagel (1980)

$$P_A \int_{\mathbb{R}} \int_{\mathbb{R}} \int_{\mathbb{L}} h(x_1, x_2, l)\, \Theta(\mathrm{d}l)\, \mathrm{d}x_1 \mathrm{d}x_2 = L_V \int_{\mathbb{R}} \int_{\mathbb{R}} \int_{\mathbb{L}} h(x_1, x_2, l) \cos\beta(l)\, \mathscr{R}(\mathrm{d}l)\, \mathrm{d}x_1 \mathrm{d}x_2, \tag{8.62}$$

where h is any nonnegative measurable function on $\mathbb{R}^2 \times \mathbb{L}$. If $\mathscr{R}$ is the uniform distribution U_1 on $\mathbb{L}$, then

$$\int \cos\beta(l) \mathscr{R}(\mathrm{d}l) = \frac{1}{2}$$

and so

$$L_V = 2P_A. \tag{8.63}$$

In this uniform case the mark distribution Θ is given by

$$\Theta(\mathrm{d}l) = 2\cos\beta(l)\, \mathscr{R}(\mathrm{d}l) = \sin 2\beta\, \frac{\mathrm{d}\beta\, \mathrm{d}\lambda}{2\pi} \qquad \text{for } 0 \le \beta < \frac{\pi}{2}. \tag{8.64}$$

As in the planar case a *rose of intersections* $P_A(l)$ can be defined: $P_A(l)$ is the intensity of the point process $\Phi \cap e_l$, where e_l is the plane perpendicular to l. Mecke and Nagel (1980) give an integral formula connecting $\mathscr{R}$ and $P_A(l)$, involving Legendre functions; see also Hilliard and Lawson (2003, pp. 157–70).

Further results on spatial fibre processes in the context of stereology can be found in Sections 10.2.2 and 10.7, and in Nagel (1983) and Zähle (1984c). Also there it is useful to apply the Steiner compact. Kiderlen and Pfrang (2005) give an example where the rose of directions and the Steiner compact are estimated for a sample of carbon fibres in pyrolytic carbon matrix. The consistency of the estimator used is shown in Kiderlen (2001) and more generally in Gardner *et al.* (2006).

A particular case is that of line processes, in particular Poisson line processes. The corresponding contact distributions are given by

$$H_B(r) = 1 - \exp\left(-\frac{L_V S(B)}{4} r^2\right) \qquad \text{for } r \ge 0 \tag{8.65}$$

for convex compact structuring element B containing the origin, and

$$H_s(r) = 1 - \exp(-\pi L_V r^2) \qquad \text{for } r \ge 0. \tag{8.66}$$

Bosan *et al.* (2003) illustrate the statistical use of the spherical contact distribution function $H_s(r)$ in the context of capillaries.

Boolean models with segments as grains are studied in many papers, in particular in the context of the material 'paper'. For applications of fibre processes to the manufacture of paper, nonwoven textiles and glass mats; see Dodson and Sampson (1999) and Sampson (2001). Provatas *et al.* (2000) leave the field of Boolean models and consider other fibre deposition models that lead to clustering of fibres.

Laslett *et al.* (1982) use a spatial segment process to model the occurrence of fission particle tracks within apatite crystals. The objective is to measure the length distribution of the tracks, and in particular to gain information about whether the distribution is unimodal or not. Since most particle tracks are revealed by etching treatment only when exposed by a sheared plane of the crystal, this is a complicated stereological problem. Numerical problems of the kind referred to in the section on planar fibre processes prevail, and it is found to be more effective to sample only the infrequent complete tracks that are revealed because of an intersection with another exposed track. The book Galbraith (2005) presents the corresponding statistical theory. These tracks provide important information about geological history.

Hanisch *et al.* (1985) use spatial fibre processes as models for systems of dislocation lines and show the value of the pair correlation function $g(r)$ for the description of such systems; see also Section 10.7.3, Stoyan and Stoyan (1986) and El-Azab *et al.* (2007). These models are Boolean models, modified Poisson line processes, and planar and spatial lattices of lines.

Fibre process models are used in the context of statistics of roots of plants. Examples include Grabarnik *et al.* (1998) and Fleischer *et al.* (2006) for the cases of maize and forest trees. Thread-like objects, so-called soil hyphae, are studied in Schack-Kirchner *et al.* (2000).

Analysis of vascular systems via fibre process is carried out in Heinzer *et al.* (2006); see also Capasso and Micheletti (2006) and Capasso *et al.* (2008).

To conclude this section, some remarks on practical *fibre length measurement* are given. There are two basic methods, which are described as follows.

(1) Use of pixel data, that is, of binary images of three-dimensional objects. Klette and Rosenfeld (2004, pp. 409–13) is a good source; see also Barber *et al.* (2003).

(2) Use of a randomly rotated and shifted (IUR, standing for 'isotropic, uniformly random') periodic grid of surfaces. The total fibre length L is estimated by

$$\hat{L} = \frac{2N}{S_V}, \tag{8.67}$$

where N is the number of intersections of fibres with surfaces and S_V the surface area of the grid per volume unit; see Baddeley and Jensen (2005). Janáček and Kubínová (2010) discuss the variance of this estimator. Čebašek *et al.* (2010) present an interesting application in microvascular research; the grid of surfaces is realised by a stack of optical sections acquired by a confocal microscope.

8.5 Surface processes

8.5.1 Plane processes

Plane processes are used as stochastic models for systems of planes in space, and can be regarded as special cases of spatial surface processes. Just as Section 8.3 used line processes to introduce fibre processes, so here the theory of plane processes is briefly reviewed as a prelude to the general theory of surface processes. As with line processes, so also plane processes can be defined as point processes in a suitable representation space; see p. 311. A Poisson plane process corresponds then to a Poisson point process in the representation space.

As in Section 8.3 the theory of random closed sets can be used to provide a theoretical framework and to introduce the notions of *stationary* and *motion-invariant* plane processes. These notions, and measure theory, tie up in a satisfactory manner with the representation space approach.

A plane process $\Phi = \{e_1, e_2, \ldots\}$ can also be described as a random measure

$$\Phi(B) = \sum_{e \in \Phi} h_2(e \cap B) \qquad \text{for all Borel sets } B \text{ of } \mathbb{R}^3, \tag{8.68}$$

where h_2 is the two-dimensional Hausdorff measure. If Φ is stationary, then one can define the *intensity* S_V of Φ to be the mean plane area per unit volume. Moreover, denote by $\mathbb{L}$ as in Section 8.4 the set of lines in $\mathbb{R}^3$ passing through the origin, a marked random measure Ψ can be defined on $\mathbb{R}^3 \times \mathbb{L}$ by

$$\Psi(B \times A) = \sum_{\{e \in \Phi:\, e^\perp \in A\}} \nu_{2,e}(e \cap B) \qquad \text{for all Borel sets } B \text{ of } \mathbb{R}^3 \text{ and } A \text{ of } \mathbb{L}, \tag{8.69}$$

where the sum is over e in Φ with normal $e^\perp$ lying in A and $\nu_{2,e}$ is the Lebesgue measure on the plane e. If Φ is stationary, then invariance arguments provide a factorisation of the intensity measure Λ of Ψ

$$\Lambda(B \times A) = S_V \cdot \nu_3(B)\, \mathscr{R}(A), \tag{8.70}$$

where $\mathscr{R}$ is a distribution on $[\mathbb{L}, \mathcal{L}]$, the *rose of (normal) directions* of Φ. If Φ is isotropic, then $\mathscr{R}$ is the uniform distribution U_1 on $[\mathbb{L}, \mathcal{L}]$. The rose of normal directions $\mathscr{R}$ can be interpreted as the distribution of the normal line to the typical plane in Φ.

If Φ is isotropic, then the mean number $\overline{n}_K$ of planes of Φ intersecting a compact convex set K is proportional to the average breadth $\overline{b}(K)$ of K:

$$\overline{n}_K = S_V \overline{b}(K). \tag{8.71}$$

As mentioned on p. 312, in the case of a Poisson plane process the number of planes intersecting K has a Poisson distribution. The contact distribution functions are

$$H_B(r) = 1 - \exp\bigl(-S_V \overline{b}(B) r\bigr) \qquad \text{for } r \geq 0 \tag{8.72}$$

and

$$H_s(r) = 1 - \exp(-2 S_V r) \qquad \text{for } r \geq 0. \tag{8.73}$$

As in the case of planar fibres, it is useful to consider the *Steiner compact* (or *associated zonoid*) S corresponding to the measure $S_V \mathscr{R}$ on $\mathbb{L}$. The Steiner compact is the symmetric compact convex set with modified support function $s_m(S, \cdot)$ given by

$$s_m(S, l) = \frac{1}{2} S_V \int_L |\langle l, l' \rangle|\, \mathscr{R}(\mathrm{d}l') \qquad \text{for } l \in \mathbb{L}, \tag{8.74}$$

where $\langle l, l' \rangle = \cos\alpha$, for α the angle between the lines l and l'.

If Φ is isotropic, then its Steiner compact S is the ball

$$S = B\left(o, \frac{S_V}{4}\right), \tag{8.75}$$

whose radius, as explained after (8.22), has dimension length^{-1}.

As in the case of planar fibre process the Steiner compact is a useful concept in the study of intersections of Φ with planes and lines. Consider for example the intersection of Φ with a fixed line l in $\mathbb{L}$. Let $P_L(l)$ be the intensity of the point process $\Phi \cap l$, also called the *rose of intersections* of Φ if considered as a function of l. Then

$$P_L(l) = 2s_m(S, l) \qquad \text{for } l \in \mathbb{L}, \tag{8.76}$$

where S is the Steiner compact of Φ.

If e is a fixed plane, then $\Phi \cap e$ is a line process with Steiner compact S_e, which is given by

$$S_e = \boldsymbol{p}_e^{\perp} S, \tag{8.77}$$

where $\boldsymbol{p}_e^{\perp}$ is the orthogonal projection onto e.

In the case of isotropy Formulae (8.76) and (8.77) give

$$P_L = \frac{1}{2} S_V, \tag{8.78}$$

where P_L is the intensity of $\Phi \cap l$, and

$$L_A = \frac{\pi}{4} S_V, \tag{8.79}$$

where L_A is the intensity of $\Phi \cap e$. Note that the left-hand sides do not depend on the particular choices of l and e.

8.5.2 General surface processes

Basic characteristics

The definition of the class of *surface processes* (or *random surfaces*) follows closely the definition of fibre processes; see Pohlmann *et al.* (1981). A *surface system* is a set ϕ contained in $\mathbb{R}^3$ which can be represented as the boundary (that is, the surface) of an $\mathbb{S}$-set A, that is, a set $A \subset \mathbb{R}^3$ in the extended convex ring. Since A is locally a finite union of convex bodies, its surface ϕ has a well-defined area measure using h_2, the two-dimensional Hausdorff measure. For a surface-like set A, which is of zero volume, $h_2(A)$ is the surface area and not the double surface area (contrast the way in which the conventions of Section 1.6 apply to spatial convex sets lying on planes). Thus the following defines, with a slight abuse of notation, for the surface system ϕ a locally finite measure, also denoted by ϕ, in $\mathbb{R}^3$:

$$\phi(B) = h_2(\phi \cap B) \qquad \text{for all Borel sets } B \text{ of } \mathbb{R}^3.$$

Let $\mathbb{Z}$ be the class of all surface systems, endowed with the σ-algebra $\mathcal{Z}$ generated by

$$\{\phi \in \mathbb{Z} : \phi(B) < x\} \qquad \text{for positive numbers } x \text{ and spatial Borel sets } B.$$

A *surface process* Φ is a random variable defined on a probability space $[\Omega, \mathcal{A}, \mathbf{P}]$ and taking values in $[\mathbb{Z}, \mathcal{Z}]$. The probability measure generated by Φ on $[\mathbb{Z}, \mathcal{Z}]$ is called the *distribution* of Φ. The surface process Φ corresponds to a random measure, the *random surface measure*; see Section 7.3.4.

Stationarity and isotropy are defined as for random closed sets or for random measures.

Stationary surface processes have two basic characteristics: a scalar, the *intensity* S_V, and a measure, the *rose of normal directions* $\mathscr{R}$. These are defined in a manner entirely analogous to the corresponding quantities for fibre processes, generalising the definitions for plane processes given in Section 8.5.1. In particular $\mathscr{R}$ gives the distribution of the normal to the typical surface point. These characteristics satisfy a *Campbell theorem* (which can be used to recover their definitions)

$$\mathbf{E}\left(\int_{\mathbb{R}^3} f\big(x, l(x)\big)\Phi(\mathrm{d}x)\right) = S_V \int_{\mathbb{R}^3}\int_{\mathbb{L}} f(x, l)\mathscr{R}(\mathrm{d}l)\,\mathrm{d}x \tag{8.80}$$

for every nonnegative measurable function f on $\mathbb{R}^3 \times \mathbb{L}$, where $l(x)$ is the surface normal at x.

If Φ is isotropic, then $\mathscr{R}$ is the uniform distribution U_1 on $\mathbb{L}$. The converse is, of course, not true. Consider, for example, a randomised lattice of non-intersecting balls and take the union of all spheres as a surface process. Then the rose of normal directions is the uniform distribution, but the surface process is anisotropic if the lattice is anisotropic. As in Sections 8.3.1 and 8.5.1, the rose of normal directions $\mathscr{R}$ can be characterised by the associated Steiner compact.

It makes sense to refine the approach by using directions of the normals, to use inward-pointing and outwarding-pointing normals. In this context one speaks about the *oriented mean normal measure*; see Kiderlen (2008) and Schneider and Weil (2008, p. 147).

Intersections by lines and planes

As in the case of fibre processes, it is of interest to consider intersections of surface processes with lines and planes. Intersection with a line generates a point process on the line; intersection with a plane produces a fibre process on the plane. (It suffices to consider plane intersections since linear intersections can be regarded as produced by first a planar intersection, and then a linear intersection of the ensuing planar fibre process. Linear intersections of planar fibre processes are dealt with in Section 8.3.2.)

Planar and linear sections of surface processes are also considered in Section 10.2, which is devoted to stereology.

Suppose that Φ is a stationary surface process and $\Phi \cap e$ is the planar fibre process resulting from the intersection of Φ with the plane e, where e is the plane $x_3 = 0$. Furthermore, let Θ be the rose of tangent directions for $\Phi \cap e$. Then Θ is connected with the rose $\mathscr{R}$ of normal directions of Φ by

$$\begin{aligned} L_A \int_{\mathbb{R}}\int_{\mathbb{R}}\int_{(0,\pi/2]} & h(x_1, x_2, \lambda)\Theta(\mathrm{d}\lambda)\,\mathrm{d}x_1\mathrm{d}x_2 \\ &= S_V \int_{\mathbb{R}}\int_{\mathbb{R}}\int_{\mathbb{L}} h\big(x_1, x_2, \lambda(l)\big)\sin\beta(l)\,\mathscr{R}(\mathrm{d}l)\,\mathrm{d}x_1\mathrm{d}x_2 \end{aligned} \tag{8.81}$$

for every nonnegative measurable function h defined on $\mathbb{R}^2 \times (0, \pi]$, where $\beta(l)$ is the azimuthal angle of l in $\mathbb{L}$, and $\lambda(l)$ is the angle of a line in e orthogonal to the projection of l onto e, and so $-\pi < \lambda(l) \leq \pi$.

If $h(x_1, x_2, \lambda) = \mathbf{1}_{[0,1]}(x_1)\mathbf{1}_{[0,1]}(x_2)$, then Formula (8.81) gives

$$L_A = S_V \int \sin\beta(l)\, \mathscr{R}(\mathrm{d}l). \tag{8.82}$$

If $\mathscr{R}$ is the uniform distribution (for example, if Φ is isotropic), then by means of Formula (8.61)

$$L_A = S_V \cdot \frac{1}{2\pi} \int_{-\pi}^{\pi} \int_0^{\pi/2} \sin^2\beta \,\mathrm{d}\beta \,\mathrm{d}\lambda = \frac{\pi}{4} S_V. \tag{8.83}$$

For the case of intersection with a line the following formula holds:

$$P_L = \frac{1}{2} S_V, \tag{8.84}$$

as in the case of a plane process. This follows from (8.83) and (8.38).

Formulae (8.76) and (8.77) for Steiner compacts remain true for general surface processes.

Intersections with fibre processes and surface processes

Hilliard (1962) discussed intersections of fibre and surface processes in $\mathbb{R}^3$ (see also Hilliard and Lawson, 2003, pp. 170–1). In particular he derived a formula for the mean number P_V of intersections per unit volume of a surface process of intensity S_V with an independent fibre process of intensity L_V, in the case of motion-invariance. The formula is

$$P_V = \frac{1}{2} L_V S_V. \tag{8.85}$$

Denote by Φ_i, $i = 1, 2$ and 3, three independent stationary and isotropic surface processes with intensities $S_{V,i}$. The intersection $\Phi_1 \cap \Phi_2$ gives a spatial fibre process with intensity

$$L_V = \frac{\pi}{4} S_{V,1} S_{V,2} \tag{8.86}$$

(Miles, 1972a; see also Hilliard and Lawson, 2003, p. 181). Combining (8.85) and (8.86) yields the intensity of the spatial point process resulted from the intersection $\Phi_1 \cap \Phi_2 \cap \Phi_3$ of three independent motion-invariant surface processes:

$$P_V = \frac{\pi}{8} S_{V,1} S_{V,2} S_{V,3}. \tag{8.87}$$

General intersection formulae are given in Wieacker (1989, Section 4) and, for the non-stationary Poisson case, in Hoffmann (2007), where the Steiner compact plays an important rôle.

Second moment measure

The definition of the *second moment measure* of a surface process follows that of a fibre process. If the surface process is stationary, then its second-order behaviour is summarised

in a reduced second moment measure, and in the isotropic case a reduced second moment function $K(r)$ suffices. The interpretation of $S_V K(r)$ is that it is the mean area of all surface pieces within a ball of radius r centred at the typical surface point.

Example 8.5. *Basic characterisations of two simple surface process models*
(a) Let Φ be an isotropic Poisson plane process with intensity S_V. By isotropy the rose of normal directions is the uniform distribution on $\mathbb{L}$. As in Example 8.4 it can be shown that the reduced second moment function $K(r)$ satisfies

$$S_V K(r) = \pi r^2 + \frac{4}{3}\pi r^3 S_V \qquad \text{for } r \geq 0.$$

(b) Let Φ be a three-dimensional Boolean disc model as in Example 8.1, with constant disc radii R. Then

$$S_V = \lambda \pi R^2,$$

where λ is the intensity of the germ process of disc centres. The reduced second moment function $K(r)$ has a more complicated form:

$$S_V K(r) = \frac{4}{3}\pi r^3 S_V + F(r) \qquad \text{for } r \geq 0,$$

where

$$F(r) = \begin{cases} \pi R^2, & \text{if } r > 2R, \\ \dfrac{2}{R^2}\displaystyle\int_0^R t f(t)\,\mathrm{d}t, & \text{if } r \leq 2R, \end{cases}$$

and $f(t) = \nu_2(B(o,r) \cap B(\boldsymbol{t}, R))$ for $\|\boldsymbol{t}\| = t$, that is, $f(t)$ is the intersection area of two discs of radii r (which comes from the ball $B(o,r)$) and R and centre distance t.

The second term comes from the disc holding the typical point while the first arises from contribution by other discs; this is reminiscent of Example 8.4.

Rough random surfaces are studied in some papers. An example is Stroeven (2000), where the surface is obtained by a planar section through a random system of balls, which generates dome-like caps and indentations of spherical particles; see Figure 8.16.

A very important tool in the context of modelling (liquid) surfaces is the *Surface Evolver*, which was developed by A. K. Brakke. It can be used to generate physically founded surfaces by energy minimisation. Information about this program can be obtained from the internet. A paper in which it is used for generating random foams is Kraynik *et al.* (2003).

The two basic methods for fibre length measurement discussed on p. 333 are also applicable for the *surface area measurement* as follows.

(1) Use of voxel data, that is, of binary images of three-dimensional objects. To estimate the surface area of such objects one determines the occurrences of certain configurations of black and white voxels in $2 \times 2 \times 2$ cubes. To each configuration type a

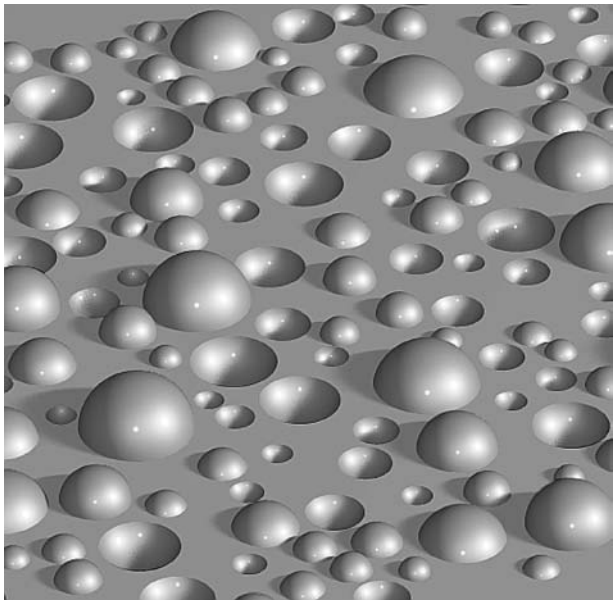

Figure 8.16 Simulated surface composed of inter-connected portions of a dividing planar section and indenting and protruding dome-like caps; see Stroeven (2000). Courtesy of M. Stroeven.

weight is assigned and the total surface area is obtained by summation of weights. See Ohser and Schladitz (2009) and Ziegel and Kiderlen (2010a,b).

(2) Use of a randomly rotated and shifted (IUR) periodic grid of lines. The total surface area S is estimated by

$$\hat{S} = \frac{2N}{L_V}, \tag{8.88}$$

where N is the number of intersections of the surface system with lines and L_V is the line length of the grid per volume unit; see Baddeley and Jensen (2005). Janáček and Kubínová (2010) discuss the variance of this estimator.

8.6 Marked fibre and surface processes

Just as for point processes, it is useful for fibre and surface processes to attach *marks* (*weights*) to the fibre and surface points constituting the process. The mark might be a real number (for example, the curvature of the fibre at the point, or its thickness if 'thick fibres' are being studied), or it might be more general; at any rate it gives further information about the structure being studied. The space of possible marks will be denoted here by $\mathbb{W}$, and it must be endowed with a σ-algebra $\mathscr{W}$.

For the case where the fibres stand for microvessels, a stereological method for the determination of fibre thickness distribution is described in Krasnoperov and Gerasimov (2003).

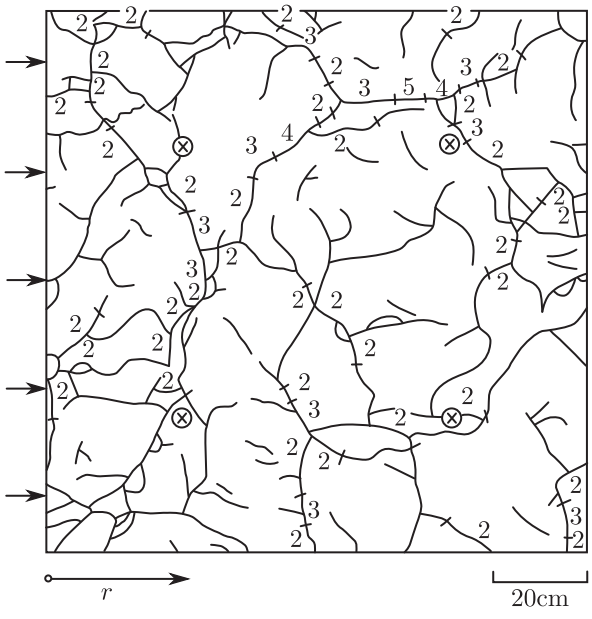

Figure 8.17 Crack pattern in a clay soil, taken from a horizontal section at depth of 30 cm (Doležal, 1982). The numbers indicate the widths of the cracks in the section plane; unlabelled cracks all have width 1 mm.

Figure 8.17 gives an example of a marked fibre process. The fibre system is the system of cracks in a clay soil on plane section. The fibres are marked by the width ('thickness') of the cracks. Note that this is indeed an intersection of a marked surface process with a plane!

As in aspects of point process theory, it can be useful to define marks for an unmarked fibre or surface process so that the marks describe distributional aspects of the process; see Stoyan (1984d). For example, the reduced second moment function $K(r)$ of a planar fibre process can be interpreted as follows: $L_A K(r)$ is the mean of a mark distribution when the mark at the typical point x is the total length $S_r(x)$ of all fibre pieces within the disc $B(x, r)$.

Mecke and Stoyan (1980a), Pohlmann *et al.* (1981) and Stoyan (1984d) gave important formulae for marked fibre and surface processes. In this section, a particular case is given a brief consideration: the case of stationary planar marked fibre processes. (Note in passing that stationarity and isotropy are defined just as in the case of marked random measures.)

The basic characteristics of a stationary planar marked fibre process are its *intensity* L_A (simply the intensity of the fibre process when the marks are disregarded) and the *joint distribution* $\mathscr{J}$ *of tangent direction and mark*. This distribution $\mathscr{J}$ can be interpreted as the joint distribution of tangent direction and mark for the typical fibre point. For L in the Borel σ-algebra Π of $(0, \pi]$ and C in $\mathscr{W}$,

$$L_A \cdot \mathscr{J}(L \times C) = \text{the mean length per unit area of all fibre fragments for which the constituent points have tangent direction in } L \text{ and mark in } C$$

(its strict definition follows closely the definition of the rose of directions, which itself can be thought of as a mark distribution). Of course,

$$\mathscr{J}(L \times \mathbb{W}) = \mathscr{R}(L) \qquad \text{for all Borel sets } L \text{ of } (0, \pi].$$

The *unconditional mark distribution* M is given by

$$M(C) = \mathscr{J}\big((0, \pi] \times C\big) \qquad \text{for all } C \text{ in } \mathscr{W}.$$

If the marked fibre process is isotropic, then $\mathscr{R}$ is uniform and $\mathscr{J}$ factorises as

$$\mathscr{J}(L \times C) = U_1(L)\, M(C) \tag{8.89}$$

Also a Campbell theorem holds, analogous to Theorem 8.3.

Intersection of a stationary marked fibre process with the x_1-axis yields a marked point process Ψ. The intersection points are marked by pairs of tangent directions and marks. Let P_L be the intensity of Ψ and $\mathscr{I}$ the joint distribution as above. Mecke and Stoyan (1980a) show that for any nonnegative measurable function h on $\mathbb{R} \times (0, \pi] \times \mathbb{W}$, it holds that

$$\begin{aligned} &P_L \int_{\mathbb{R}} \int_{(0,\pi]\times\mathbb{W}} h(x, \alpha, w)\mathscr{I}\big(\mathrm{d}(\alpha, w)\big)\, \mathrm{d}x \\ &\quad = L_A \int_{\mathbb{R}} \int_{(0,\pi]\times\mathbb{W}} h(x, \alpha, w) \sin\alpha\, \mathscr{J}\big(\mathrm{d}(\alpha, w)\big)\, \mathrm{d}x. \end{aligned} \tag{8.90}$$

In the case of isotropy

$$\mathscr{I}\big(\mathrm{d}(\alpha, w)\big) = \frac{1}{2} \sin\alpha\, \mathrm{d}\alpha\, M(\mathrm{d}w). \tag{8.91}$$

Thus in the isotropic case the mark distribution $\mathscr{I}$ also factorises. One factor is the mark distribution M and the other the angle distribution given by Formula (8.39).

Example 8.6. *Cracks in clay soil (Doležal, 1982; Sandau, 1993; Sandau and Vogel, 1993)* Figure 8.17 shows a pattern of cracks in soil in planar section. Doležal (1982) uses stereological methods to draw inferences about the spatial crack structure. Here the planar fibre system is considered as a marked fibre process, with marks being the crack widths as shown in Figure 8.17.

Length measurements yield an estimate for L_A of $\hat{L}_A = 0.134\,\mathrm{cm}^{-1}$, using Formula (8.54). Line and circle section methods were also used to estimate L_A. The arrows in

Table 8.1 Empirical (mark) distributions for the crack-width.

Width (mm)	Exhaustive measurement	Line section method	Circle section method
1	0.786	0.783	0.770
2	0.163	0.174	0.203
3	0.039	0.043	0.027
4	0.009	0	0
5	0.004	0	0

Figure 8.17 define five line segments parallel to the bottom line of the window, and if these are used as test set and if isotropy is assumed, then Formula (8.55) yields $\hat{L}_A^{\text{segment}} = 0.120\,\text{cm}^{-1}$. The circle section method used four circles of radius $r = 30\,\text{cm}$ and centres at the points marked in Figure 8.17 by $\otimes$. Formula (8.56) yields $\hat{L}_A^{\text{circle}} = 0.154\,\text{cm}^{-1}$. This example may be instructive in illustrating actual errors of measurement.

Using both line and circle methods, marks were measured for the intersection points. The corresponding empirical distributions are tabulated in Table 8.1, together with the distributions of marks obtained by exhaustive length measurement.

This approach is greatly refined in Sandau (1993), who considers the three-dimensional problem and studies a stationary marked surface process. By means of vertical sections Sandau (1993) and Sandau and Vogel (1993) determine the joint distribution of spatial direction and width of the cracks.